REVIEW

Innate immune evasion mediated by picornaviral 3C protease: Possible lessons for coronaviral 3C-like protease?

Chen Seng Ng[1,2] | Christopher C. Stobart[3] | Honglin Luo[1,2]

[1]Centre for Heart Lung Innovation, St Paul's Hospital, University of British Columbia, Vancouver, Canada

[2]Department of Pathology and Laboratory of Medicine, University of British Columbia, Vancouver, Canada

[3]Department of Biological Sciences, Butler University, Indianapolis, Indiana, USA

Correspondence
Honglin Luo, Centre for Heart Lung Innovation, and Department of Pathology and Laboratory of Medicine, University of British Columbia-St. Paul's Hospital, Room 166, 1081 Burrard Street, Vancouver, BC, V6Z 1Y6, Canada.
Email: honglin.luo@hli.ubc.ca

Summary

Severe acute respiratory syndrome coronavirus-2 is the etiological agent of the ongoing pandemic of coronavirus disease-2019, a multi-organ disease that has triggered an unprecedented global health and economic crisis. The virally encoded 3C-like protease (3CL^{pro}), which is named after picornaviral 3C protease (3C^{pro}) due to their similarities in substrate recognition and enzymatic activity, is essential for viral replication and has been considered as the primary drug target. However, information regarding the cellular substrates of 3CL^{pro} and its interaction with the host remains scarce, though recent work has begun to shape our understanding more clearly. Here we summarized and compared the mechanisms by which picornaviruses and coronaviruses have evolved to evade innate immune surveillance, with a focus on the established role of 3C^{pro} in this process. Through this comparison, we hope to highlight the potential action and mechanisms that are conserved and shared between 3C^{pro} and 3CL^{pro}. In this review, we also briefly discussed current advances in the development of broad-spectrum antivirals targeting both 3C^{pro} and 3CL^{pro}.

KEYWORDS
Covid-19, picornaviruses, SARS-CoV-2, 3C^{pro}, 3CL^{pro}

1 | INTRODUCTION

Coronavirus disease-2019 (Covid-19) is a multiple organ disease that has posed an unprecedented health and economic threat worldwide since its emergence in late 2019. Covid-19 is caused by a novel virus strain,[1,2] namely severe acute respiratory syndrome-coronavirus-2 (SARS-CoV-2)[3], categorized within the family *Coronaviridae*. It can infect various hosts and target multiple organs through the body.[4] Coronaviruses are a family of enveloped, single-stranded RNA (ssRNA) viruses with positive polarity that can cause respiratory, enteric, cardiovascular, and central nervous system diseases.[5,6] This family of RNA viruses features the second largest genome size (27–31 kb) found to date right after planarian nidovirus (∼41.1 kb).[7] Together with SARS-CoV and Middle East Respiratory Syndrome-CoV (MERS-CoV) that caused SARS and MERS outbreaks in 2003 and 2012, respectively, SARS-CoV-2 belongs to the genus *betacoronavirus*. The genome of *betacoronavirus* encodes more than 20 proteins, including four major structural proteins (i.e., a spike (S) protein that binds to the cell receptor and mediates fusion between virus and cell membrane, a small envelope (E) protein, a highly hydrophobic membrane (M) protein, and a nucleocapsid (N) protein that interacts with viral RNA to form a helical nucleocapsid structure), two cysteine proteases (i.e., a papain-like cysteine protease (PL^{pro}) and a 3-chymotrypsin-like cysteine protease (3CL^{pro}, also known as the main protease, M^{pro}) that processes viral polyproteins into individual functional proteins, a helicase required for unwinding double-stranded RNA (dsRNA), a RNA-dependent RNA polymerase (RdRp) that catalyzes the replication of RNA from RNA template, and other enzymes such as endo- and exonucleases essential for viral nucleic acid metabolism.[8]

Among these proteins, SARS-CoV-2 proteases play a vital role in viral replication and transcription, thereby being recognized as attractive antiviral targets for Covid-19 treatment.[9,10] Of the two known CoV proteases that are encoded by open reading frame 1a (ORF1a), 3CL^{pro} [corresponding to nonstructural protein 5 (NSP5)], which is highly conserved among all CoV 3CL^{pro}, has been identified to be structurally analogous to the 3C^{pro} of picornaviruses (3CL^{pro} is named after the picornaviral 3C^{pro}).[11,12] Despite subtle structural differences in the active sites, 3CL^{pro} and 3C^{pro} share a similar chymotrypsin-like tertiary structure with a catalytic triad (or dyad) site containing a cysteine nucleophile (Figure 1). Moreover, both of the enzymes have a strong preference for glutamine (Gln) at the P1 position of their targets, the most key determining factor for their substrate recognition. The conserved active sites of 3C^{pro} and 3CL^{pro} have been confirmed by high-resolution three-dimensional structural analysis. Therefore, it is proposed to serve as an attractive target for the design of broad-spectrum antiviral drugs.[13–15] Picornaviruses are small, non-enveloped viruses containing a positive-sense, ssRNA genome with a length of 7.0–8.5 kb. This family comprises 29 genera, including *Apthovirus* (e.g., foot-and-mouth disease virus, FMDV), *Cardiovirus* (e.g., encephalomyocarditis virus, EMCV), *Enterovirus* (e.g., poliovirus, PV; coxsackievirus A16/B3, CVA16; CVB3; enterovirus-A71/D68; EV-A71; EV-D68), *Rhinovirus* (e.g., human rhinovirus, HRV),

and *Hepatovirus* (e.g., hepatitis A virus, HAV) genera.[16] Picornavirus genomic RNA at its 5′ end is covalently linked to a small viral protein (VPg, also known as 3B) that serves as a primer for the initiation of viral RNA replication. Further, instead of a cap structure, the genome of picornaviruses possesses an element termed internal ribosome entry site (IRES) in their 5′-untranslated region (UTR), which is necessary for initiating a cap-independent translation of viral RNA. The viral genome of picornaviruses contains one open reading frame encoding a single viral polyprotein that undergoes proteolysis by two viral proteases, 2A^{pro} and 3C^{pro}, with the latter being responsible for the majority of the maturation cleavage events of viral polyprotein similar to coronaviral 3CL^{pro}[17]. In addition to processing viral polyprotein, picornaviral proteases also target cellular proteins to evade the human immune surveillance and facilitate viral infection.[18]

Given the common characteristics of 3C^{pro} and 3CL^{pro}, we postulate that SARS-CoV-2, like picornaviruses, is capable of regulating host innate antiviral processes through the catalytic activity of its 3CL^{pro}. The delay or inhibition of multiple host antiviral machineries would allow effective viral growth and subsequently optimal release and infection. Here we will recapitulate some of the scenarios on how picornaviruses utilize its 3C^{pro} to target major host antiviral mechanisms.

1.1 | Structural and functional similarities between picornaviral 3C^{pro} and coronaviral 3CL^{pro}

Early during the viral replication cycle, the positive-sense ssRNA (+ssRNA) genomes of picornaviruses and coronaviruses are translated into one or more polyproteins, which include integrated viral protease domains. Maturation cleavage events mediated by virally encoded proteases in both backgrounds are indispensable for virus replication. The picornaviral 3C^{pro} (working in concert with the 2A^{pro}) mediates the majority of viral cleavage events including autocleavage from the 3D polymerase (3D^{pol}) domain of the virus. Similarly, coronaviral 3CL^{pro} is responsible for at least 11 maturation cleavages of the viral replicase polyproteins, including its own autoproteolytic cleavage. Beyond these requisite viral polyprotein cleavages, both 3C^{pro} and 3CL^{pro} target and cleave host cellular proteins. Due to the importance in their respective viral backgrounds, these proteases have been extensively studied as primary targets for viral inhibition for over 30 years.

The picornaviral 3C^{pro} is a chymotrypsin-like cysteine protease comprised of two β-barrel domains of six antiparallel strands which surrounds a conserved Cys-His-Asp/Glu catalytic triad (Figure 1).[19,20] The protease preferentially cleaves after a P1-Gln with greater cleavage site variability in the other cleavage site residue positions.[21] During picornaviral replication, the 3CD^{pro} precursor, which is able to process the P1 structural precursor but lacks polymerase activity, is cleaved to release 3C^{pro} and viral RdRP 3D^{pol}[22]. The conversion of 3CD^{pro} to 3C^{pro} plays a critical role in facilitating the transition and regulation from viral translation to replication.[23,24] Structurally and functionally analogous to the picornaviral 3C^{pro}, the coronaviral
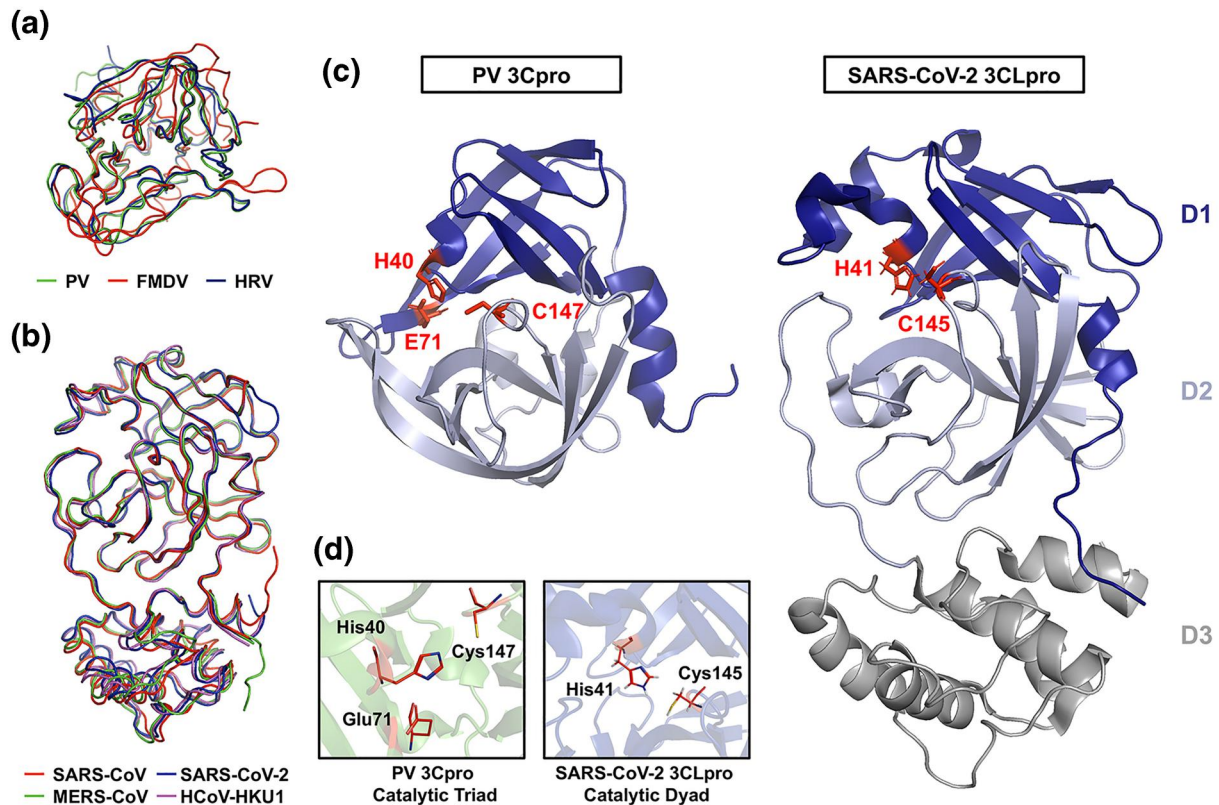
FIGURE 1 Crystal structures and superposition of picornaviral 3C protease (3C^pro) and coronaviral 3C-like protease (3CL^pro). (a) Ribbon overlay of the picornaviral 3C^pro structures of poliovirus (PV; PDB 1L1N), foot-and-mouth disease virus (FMDV; PDB 2BHG), and human rhinovirus (HRV; PDB 1CQQ). (b) Ribbon overlay of human coronaviral 3CL^pro structures of severe acute respiratory syndrome-coronavirus (SARS-CoV; PDB 2Q6G), Middle East Respiratory syndrome-CoV (MERS-CoV; PDB 4YLU), SARS-CoV-2 (PDB 6M2N), and HCoV-HKU1 (PDB 3D23). (c) A side-by-side comparison of PV 3C^pro and SARS-CoV-2 3CL^pro with the two domains of the chymotrypsin-like fold highlighted and the active site catalytic residues labeled and highlighted (red). (d) Close-up images of the active site catalytic residues of PV 3C^pro and SARS-CoV-3CL^pro are shown

3CL^pro is an approximately 300 residue, 3-domain protease. Domains 1 and 2 comprise the substrate-binding and enzymatic active sites of the protease with dimerization driven by interactions between the structurally unique and largely helical domain 3.[25,26] Domains 1 and 2 of 3CL^pro form a chymotrypsin-like fold comprised of antiparallel β-barrels housing the His-Cys catalytic dyad residues.[26,27] The antiparallel β-barrel conformation within domains 1 and 2 surrounding and forming the active site of 3CL^pro shares structural similarity to the core structure of the picornaviral 3C^pro, albeit with subtle differences in strand positioning (Figure 1). Unlike the picornaviral 3C^pro (monomer with only two catalytic domains), an attached helical third-domain in 3CL^pro facilitates dimerization of the protease, an essential event for its enzymatic activity and viral replication (Figure 1C, Domain 3).[28] While targeting the third domain of 3CL^pro serves as a valid strategy to disrupt its dimerization and catalytic activity, any inhibitors identified or designed to do so likely have no impact on picornaviral 3C^pro activity since dimerization is not necessary for its function. In addition, among coronaviruses, there is considerably more structural conservation for the chymotrypsin-like fold of 3CL^pro compared to that of the picornaviral 3C^pro. Based on large part to their structural and functional similarities between the

3C^pro and 3CL^pro, it remains unclear to what extent these proteases share common host cellular targets during viral replication and what role these potentially shared cleavages play in viral replication.

2 | THE SUBVERSION OF HOST DEFENSE MECHANISMS BY picornaviral 3C^pro

2.1 | Targeting type I interferon signaling pathway

The effectiveness of an antiviral innate immunity depends on the accurate recognition of viral moieties, known as the pathogen-associated molecular patterns (PAMPs), by pattern-recognition receptors (PRRs) composed of at least three classes: retinoic acid-inducible gene-I (RIG-I)-like receptors (RLRs), Toll-like receptors (TLRs), and nucleotide-binding oligomerization domain (NOD)-like receptors (NLRs).[29] Upon RNA viral infection, dsRNAs often accumulate in cells in the form of the viral genome or its replication intermediates. The dsRNAs can be recognized by cytosolic viral RNA sensor, RLRs (e.g., RIG-I (encoded by *Ddx58* gene) and melanoma differentiation-associated proteins (MDA5, encoded by *Ifih1* gene)), and/or endosomal

viral RNA sensor (e.g., TLR3) to initiate type I interferon (IFN-I) immune response. While RIG-I preferentially binds to shorter dsRNA (<1-2 kb) bearing 5′-triphosphate group, MDA5 primarily recognizes long dsRNA.[30] Similar to picornavirus, SARS-CoV-2 has a long RNA genome. It is therefore expected that SARS-CoV-2 RNA favorably binds to MDA5 rather than its paralog RIG-I. Indeed, MDA5 has been previously shown to be the specific PRR that recognizes murine coronavirus RNA.[31] Interaction between viral RNA and MDA5 forms MDA5 filaments along dsRNAs, which brings together neighboring caspase activation and recruitment domain (CARD) in close proximity to induce oligomerization and activation of the adapter mitochondrial-antiviral signaling protein (MAVS).[32] Activated MAVS then transmits the signals to its downstream transcription factors, interferon regulatory factor-3/7 (IRF3/7) and nuclear-factor-κB (NF-κB), through TANK-binding kinase-1 (TBK1) and IκB kinase-ε (IKKε). The homo- or hetero-dimerized IRF3/7 subsequently translocate to the nucleus and induce the expression of IFN-I-associated genes (*Ifna* and *Ifnb1*), which could further activate the Janus kinase/signal transducers and activators of transcription (JAK/STAT) signaling cascade to trigger the expression of antiviral genes, called interferon-stimulated genes (ISGs).[30] Please see Figure 2 for the details.

To antagonize human antiviral innate immune response, picornaviruses target critical components of the RLR signaling pathway for degradation. It was reported that infections with Seneca Valley virus (SVV), PV, EV-A71, EV-D68, CVB3, CVA16, CVA6, HRV-1A, EMCV, and HAV cleave MDA5, MAVS, RIG-I, IRF7, and/or IRF9 through the actions of 3C[pro], leading to a disruption of RLR-mediated IFN-I immune responses.[33–39] In addition to 3C[pro], studies have found that MDA5 and MAVS can also be targeted by 2A[pro] upon PV, EV-A71, CVB3, and HRV-1A infections.[34,40,41] Moreover, both TAK1 binding protein-1 (TAB1) and NF-κB essential modulator (NEMO, an adapter protein bridging the canonical IKKα/β kinases and the noncanonical kinases TBK1/IKKε via the TANK adapter[42]) are cleaved by 3C[pro] following EV-A71, FMDV and HAV infections, resulting in reduced production of IFN-I.[43–45] In addition, FMDV utilizes its 3C[pro] to inhibit STAT2 function, a component of the IFN-stimulated gene factor 3 complex, which is also mirrored by the 3CL[pro] of PDCoV (Table 1, *yellow highlighted row*).[57,58] Another interesting finding associated with this topic is 3C[pro]-induced cleavage of Toll/IL-1 receptor (TIR)-domain-containing adapter-inducing interferon-β (TRIF) during CVB3, EV-A71, and HAV infections.[36,47,48] TRIF is an adapter protein mediating type I IFN antiviral response downstream of the endosomal TLR3 (a viral RNA sensor)[114] and cleavage causes the loss of its function in host defense.

In addition to directly targeting components of the IFN-I pathway, 3C[pro] can also modulate the function of proteins that participate in the regulation of this pathway. For instance, the 3C[pro] of EV-A71 downregulates miRNA-526a, consequently leading to increased expression of cylindromatosis (CYLD, a target of miRNA-526a).[115] CYLD is a deubiquitinating enzyme negatively regulating the function of RIG-I by removing K63-linked polyubiquitin chains from RIG-I.[116] Ubiquitination is a post-translational modification required for RIG-I activation,[117] and deubiquitination results in its

inactivation. Together, available evidence reveals that 3C[pro] plays a key role in the efforts of picornaviruses in counteracting the host antiviral immune response by cleaving or inactivating essential adapter proteins in the RIG-I/MDA5-MAVS and/or the TLR3-TRIF signaling pathways (Figure 2).

Like picornaviruses, both SARS-CoV and MERS-CoV trigger a limited IFN-I response.[118–120] A mouse model infected with SARS-CoV demonstrated that a significant delay in IFN production contributes to disease progression and severity.[121] Using different model systems including cells and ferrets infected with SARS-CoV-2 and post-mortem lung tissues from COVID patients, a recent study showed that SARS-CoV-2 infections elicit low levels of IFN-I and no activation of TBK1 and ISGs.[122] Of note, it was found that SARS-CoV-2 is highly sensitive to IFN-I, suggesting an important role for IFN-I in antiviral defense.[122,123] Although experimental data on SARS-CoV-2 is still limited, current evidence from SARS-CoV and MERS-CoV research revealed that CoVs develop different strategies to overcome the host innate immunity. For example, the PL[pro] of SARS-CoV, which has deubiquitinating activities, acts as an IFN-I antagonist by removing ubiquitin chains from IRF3 and through preventing the phosphorylation of IRF3[124,125]. It was also discovered that the ORF3b, ORF6, and N proteins of SARS-CoV inhibit production and action of IFN-I.[126] Moreover, M protein of SARS-CoV was shown to physically associate with RIG-I, TBK1, IKKε, and TRAF3 and inhibit gene transcription of IFN-I.[127] Most interestingly, several coronaviruses, including SARS-CoV-2, porcine deltacoronavirus (PDCoV), and porcine epidemic diarrhea virus (PEDV) have been reported to cause the cleavage of TAB1 or NEMO through their individual 3CL[pro] (Table 1, *yellow highlighted row*),[49,59,60] suggesting an important role for 3CL[pro] in antagonizing the host antiviral innate immune response.

The importance of virus-induced cytoplasmic aggregates, termed antiviral stress granules (avSGs),[128] in RLRs-mediated innate immunity has been increasingly recognized. Upon viral infection, dsRNAs are generated and accumulate in the cytoplasm, which activate the viral RNA sensor protein kinase R (PKR) and cause phosphorylation of eukaryotic initiation factor 2α and consequent formation of avSGs. Together with key molecules (i.e., Ras-GTPase-activating protein SH3 domain-binding protein 1 (G3BP1) and T cell intracellular antigen 1), avSGs are formed by recruiting multiple antiviral effectors, such as RLRs, Pumilio, DEAH-box helicase 36, Mex-3 RNA binding family member C, tripartite motif containing 25, OAS and RNaseL.[128–132] The close-proximity of 5′-triphosphate containing ssRNA and dsRNA with RLRs within the compact avSG compartment facilitates a more robust RLR-mediated IFN-I responses to suppress viral replication.[128–132] To bypass this, picornaviruses, including PV, EMCV, CVB3, FMDV, and EV-D68, utilize 3C[pro] to cleave G3BP1 and block avSG formation to prolong viral survival.[108–111,133]

CoVs were also found to be able to modulate the formation of avSGs. It was reported that MERS-CoV accessory protein 4a prevents PKR activation by directly binding viral dsRNA, thereby inhibiting avSG formation allowing for effective viral replication.[134,135] However, the role of protein 4a in avSG formation
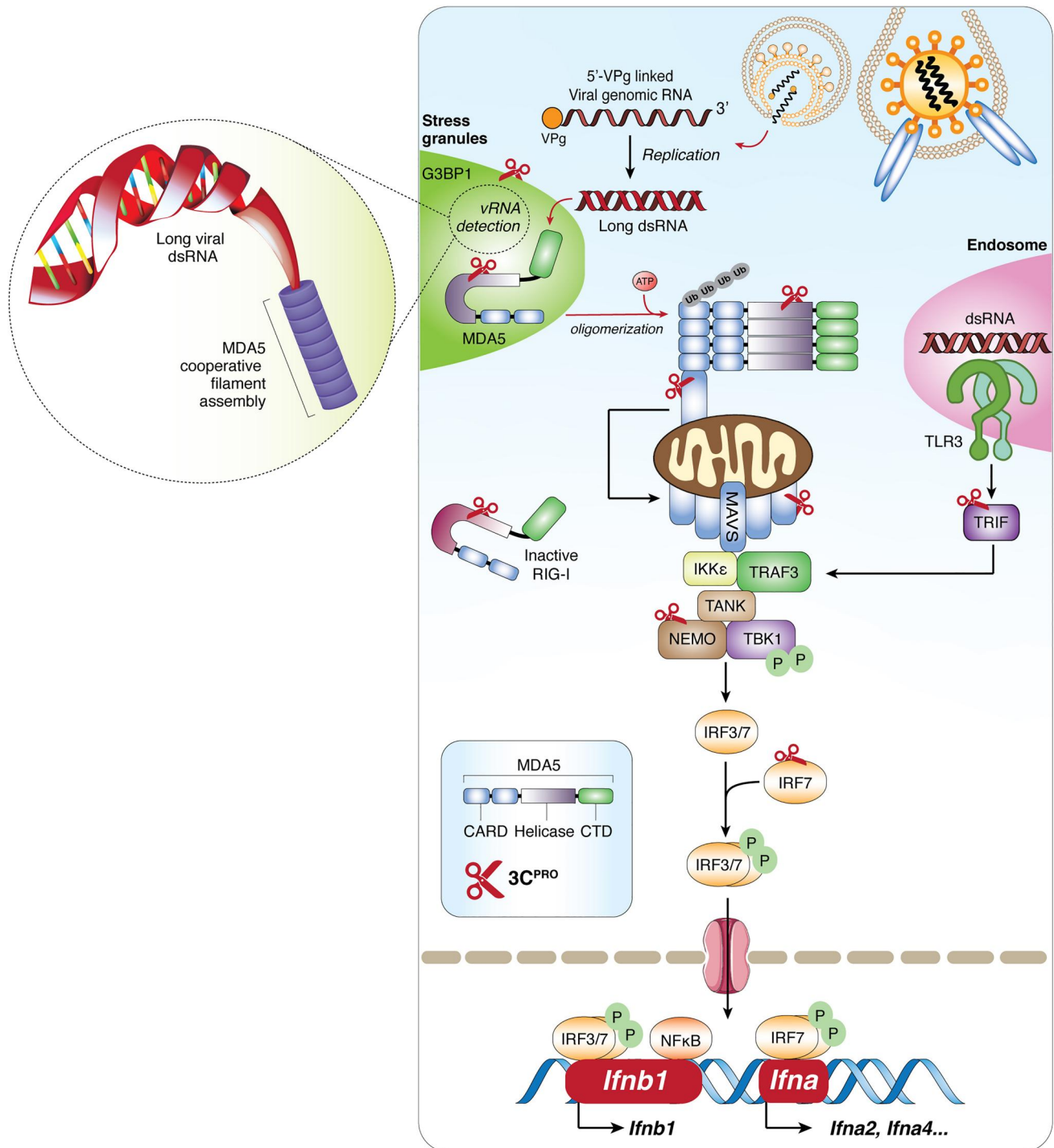
FIGURE 2 Picornaviruses evade type I interferon immune response via the function of 3C protease (3C^pro). Binding of picornaviruses to their respective receptors facilitates their entry into the cells and release of the 5′-viral protein genome-linked-containing genomic RNA into cytoplasm. Long double-stranded RNA generated during the replication process binds to MDA5, exposing its CARD and allowing homotypic CARD-CARD interactions with its downstream adapter, MAVS. Subsequently, MAVS triggers the expression of IFN-I genes (*Ifnb1* and *Ifna* in dendritic cells) and ISGs for antiviral purposes through the activation of transcription factor IRF3/7 and NF-κB. To facilitate a robust signaling, more efficient detection of dsRNA occurs in antiviral stress granules. Targets of viral encoded 3Cpro are indicated. CARD, caspase activation and recruitment domain; CTD, C-terminal binding domain; G3BP1, Ras GTPase-activating protein-binding protein 1; IFN-I, type-I interferon; IKKε, inhibitor of nuclear factor-κB (IκB)-kinase-ε; IRF3/7, interferon regulatory factors-3/7; ISGs, interferon-stimulating genes; MAVS, mitochondrial antiviral signaling protein; MDA5, melanoma-differentiation associated protein-5; NF-κB, nuclear factor-κB; NEMO, NF-κB essential modulator; P, phosphate-group; RIG-I, retinoic acid-inducible gene-I; TBK1, TANK binding kinase-1; TLR3, Toll-like receptor 3; TRAF3, TNF-receptor associated factor-3; TRIF, Toll/IL-1 receptor domain-containing adapter-inducing interferon-β

TABLE 1 Picornaviruses and coronaviruses proteinase targets [Correction added on 17 February 2021, after first online publication. Table 1 was updated in this version.]

	Proteinase	Virus	Gene symbol	Full gene name	Cleavage site	Implication to host	Ref
Host defense and inflammation	3C	CVB3, RV, PV, EV-A71, SVV	RIG-I	Retinoic acid-inducible gene-I	N/A	Dampened cytokines production; enhanced viral propagation	33,39
	2A	PV, EV-A71, CVB3	MDA5	Melanoma differentiation-associated protein 5	N/A		37,40
	2A, 3C, 3CLSP	CVB3, HRV, EV-A71, PV, SVV, PRRSV	MAVS	Mitochondrial antiviral signaling	Q148↓, Q209↓, Q251↓, Q265↓, Q268↓		34,36,38,40,41,46
	3C	EV-D68, EV-A71, CVB3, HAV, SVV	TRIF	TIR domain-containing adapter inducing interferon beta	Q159↓, Q190↓, Q312↓, Q554↓, Q653↓		36,47,48
	PL	SARS-Cov-2	IRF3	Interferon regulatory factor 3	G270↓		49
	3C	EV-D68, EV-A71	IRF7	Interferon regulatory factor 7	Q167↓, Q189↓		35,50
	3C	EV-A71	IRF9	Interferon regulatory factor 9	N/A		51
	2A, 3C	EV-A71, CVB3	NLRP3	NACHT, LRR, and PYD domain-containing protein 3	Q225↓226G, G493↓494L		52,53
	3CL	SARS-Cov-2	NLRP12	NACHT, LRR, and PYD domain-containing protein 12	Q238↓, Q938↓		49
	3C	EMCV, SVV	TANK1	TRAF family member-associated NF-κB activator-1	E272 and Q291		54
	2A	EV71	IFNAR	Interferon alpha and beta receptor subunit 1	N/A		55
	3C	HRV, PV	C3	Complement C3	N/A		56
	3C, 3CL	FMDV, PDCoV	STAT2	Signal transducer and activator of transcription 2	Q685↓, Q758↓		43,44,57–61
	3C, 3CL, 3CLS	FMDV, HAV, PEDV, PRRSV	NEMO	NF-κB essential modulator	Q304↓, Q383↓, Q231↓, E349↓350S		
	3C	EV-D68, EV-A71, CVA6, CVA16	TAK1	Transforming growth factor-β-activated kinase 1	Q360↓361S		37,45,49
	3C, 3CL	EV-A71, SARS-CoV-2	TAB1	TAK1 binding protein 1	Q414↓415G, Q451↓452S, Q132↓133S, Q444↓445S		
	3C	EV-A71	TAB2	TAK1 binding protein 2	Q113↓114S		
	3C	EV-A71	TAB3	TAK1 binding protein 3	Q173↓174G, Q343↓344G		
	3C	CVB3, PV	RIP1, RIP3	Receptor interacting protein-1, -3	Q134↓, Q430↓, R118↓119I		62,63
	3C	EV-A71	ZAP	Zinc-finger antiviral protein	Q369↓370G		64
	3C	EV-A71	GSDMD	Gasdermin-D	Q193↓194G	Inhibition of pyroptosis & promotion of viral growth	65
Autophagy	2A	CVB3	p62/SQSTM1	Sequestosome-1	G241↓	Disruption of cellular autophagy pathway	66–70
	2A	CVB3	NBR1	Neighbor of BRCA1 gene	G402↓, E682↓		
	3C	CVB3	CALCOCO2/NDP52	Calcium binding and coiled-coil domain containing protein-2; Nuclear dot 10 protein 52	Q139		
	3C	CVB3	SNAP29	Synaptosomal-associated protein 29	Q161↓		
	3C	CVB3	PLEKHM1	Pleckstrin homology domain and RUN domain Containing M1	Q668↓		

TABLE 1 (Continued)

	Proteinase	Virus	Gene symbol	Full gene name	Cleavage site	Implication to host	Ref
Cellular Integrity	2A	CVB3	DYSF	Dysferlin	N/A	Disruption of muscle membrane repair	71
	2A	CVB3, CVB4	DMD	Dystrophin	*Human*: (G589↓; G2,435↓) *Mouse*: (G591↓; G2,428↓)	Muscular dystrophy, especially heart muscle	72
	2A	HRV2	CK-II	Cytokeratin K8	G15↓	Disruption of cytoplasmic cytoskeleton	73
	3C	PV	MAP-4	Microtubule-associated protein 4	Q188↓189G	Collapse of microtubules, disruption of host protein dynamics and interactions	74
Transcription	3C	PV	Oct-1	Octomer binding transcription factor-1	Q330↓331G	Disruption of polymerase activity, affecting gene transcription	75
	3C	PV	La/SSB	Lupas autoantigen/Sjogren syndrome antigen B	Q358↓359G		76
	2A	PV	TBP	TATA-binding protein	Q18↓19G, Q104↓105S		77–80
	3C	PV	TFIIIA/C	Transcription factor for polymerase III A	N/A		81,82
	3C	PV	CREB	cAMP response element-binding protein	Q172↓173G		
	2A	CVB3	SRF	Serum response factor	G327	Disruption of SRF-dependent gene expression (e.g. cardiac contractile and regulatory factors)	83
	3C	PV	PTB/p52/hnRNAP-I	Polypyrimidine tract-binding protein	Q148/152/321A	Disruption of normal RNA metabolism (e.g. splicing)	84
	3C	PV	hnRNP M, K	Heterogenous nuclear ribonucleoprotein M, K	G389↓390E, Q364↓365G		85
	2A	PV	Gemin3	Gemin3	G463↓		86
	3C	CVB3	TDP-43	Transactive response DNA-binding protein-43	Q327↓328A		87
	3C	PV	p65-RelA	Nuclear factor (NF)-κB p65 subunit	Q480↓481G	Disruption of p65-dependent gene expression	88

(Continues)

TABLE 1 (Continued)

	Proteinase	Virus	Gene symbol	Full gene name	Cleavage site	Implication to host	Ref
Translation and RNA turn over	3C	CVB3	AUF1	(AU)-rich element RNA-binding factor 1	N/A	Disruption of host mRNA turn over	89
	2A, 3C	PV, CVB3, HAV, EMCV, FMDV, DHAV	PABP	Poly(A)-Binding protein	Q537↓, Q367↓368G, M487↓, G488↓, Q437↓438G	Host protein translation shut-off, disruption of SG formation	90–93
	3C	FMDV	eIF4A	Eukaryotic elongation factor 4A	G674↓675R, R481↓482G		94–99
	L, 2A, 3C	FMDV, PV, CVB3, EV-A71, RV	eIF4G-I, -II	Eukaryotic elongation factor 4G-I/4G-II			
	3C	PV, CVB3, HRV	eIF5B	Eukaryotic elongation factor 5B	Q478↓479G		100
	2A	CVB3	DAP5	Death-associated protein 5	G434↓		101
	3C	PV	PCBP2	Poly(rC)-binding protein-2	Q253↓, Q306↓, S254↓		102
	3C	PV	DCP1a	mRNA-decapping enzyme 1A	N/A	Disruption of P-body foci; disruption of 5′→3′ guanosine cap removal and Xrn1-Dcp1-dependent antiviral pathway	103
Others	3C	CVB3	IKBα	Inhibitor of κBα	Q249↓250G	Constitutive activation of NFκB and apoptosis	104
	2A, 3C	CVB3	GAB1	Growth factor receptor bound 2-associated binding protein-1	G175↓, G436↓, G238↓	Disruption the assembly of protein complexes for intracellular signaling	105
	2A	HRV, PV	Nup62, Nup98, Nup153,	Nucleoporins	A103↓, G177↓, G201↓, G218↓, G247↓, A298↓,	Temporal blocking of nucleocytoplasmic trafficking	106,107
	L, 3C	CVB3, PV, EMCV, FMDV, ERAV	G3BP1, G3BP2	Ras-GTPase activating-SH3-binding protein-1	Q325↓, E284↓	Disruption of SG and innate immune response	108–113
	3C	CVB3, PV	GBF1	Golgi-specific brefeldin A-resistance guanine exchange factor-1	Q1,297↓1298S	Disruption of host secretory pathway	63
			ACLY	ATP citrate lyase/synthase	Q777↓778A	Disruption of fatty acid biosynthesis	
			p115/USO1	General vesicular transport factor p115	Q832↓833G	Disruption of the host peripheral membrane recycling process between cytosol and Golgi	
			ALIX/PDCD6IP	Programmed cell death 6-interacting protein	Q728↓729S	Disruption of cellular apoptosis	
			PFAS	Phosphoribosylformylglycinamidine synthetase	Q472↓473G	Disruption of host ATP, and L-glutamine biosynthesis	

Abbreviations: CVA6/A16/B3, Coxsackievirus-A6/A16/B3; CALCOCO2, coiled-coil domain-containing protein 2; DHAV, duck hepatitis A virus; EMCV, encephalomyocarditis virus; ERAV, equine rhinitis A virus; FMDV, foot-and-mouth disease virus; GBF1, golgi-specific brefeldin A-resistance guanine nucleotide exchange factor; GBF1, Ras-GTPase-activating SH3 domain binding protein 1; GSDMDM, gasdermin D; HAV, hepatitis A virus; HRV, human rhinovirus; hnRNP M/K, heterogeneous nuclear ribonucleoprotein M/K; MAVS, mitochondrial antiviral signaling protein; MDA5, melanoma differentiation-associated protein-5; NDP52, nuclear dot 10 protein 52; NBR1, neighbor of *BRCA1*; NLRP3, NLR family PYD containing protein-3; NEMO, NF-κB essential modulator; NF-κB, nuclear factor-κB; PDCoV, porcine deltacoronavirus; PEDV, porcine epidemic diarrhea virus; PFAS, phosphoribosylformylglycinamidine synthetase; PLEKHM1, pleckstrin homology domain and RUN domain containing M1; PRRs, pathogen recognition receptors; PRRSV, porcine reproductive and respiratory syndrome virus; RIP1, receptor-interacting serine/threonine-protein kinase 1; SARS-CoV-2, severe acute respiratory syndrome coronavirus-2; SSV, Seneca Valley virus; STAT2, signal transducer and activator of transcription 2; TAB1, TAK1 binding protein-1; TRIF, (TIR)-domain-containing adapter-inducing interferon-β

Note: Color coding correspond between virus and cleavage site)

appears to be cell type-specific. MERS-CoV mutant with deletion of 4a gene still impedes avSG formation in certain cell types,[134,135] suggesting that additional proteins (possibly viral proteases) encoded by MERS-CoV are required to antagonize avSGs. In a recent report, Grogan and colleagues[8] utilized an affinity purification mass spectrometry proteomics approach to screen for cellular proteins that interact with individual SARS-CoV-2 proteins, including 3CL^pro. Using both wild-type and catalytically inactive (C145A) 3CL^pro, they identified two high-confidence interactions with the histone deacetylase 2 (HDAC2) and tRNA methyltransferase 1 (TRMT1), respectively. Of interest, HDAC2 has been previously shown to be required for IFN-I signaling through histone modification.[136,137] Remarkably, in addition to 3CL^pro, other SARS-CoV-2-encoded proteins were also found to interact with cellular proteins involved in regulating host innate immunity, including the core avSG protein G3BP1[8], a known antiviral protein that induces the innate immune response.[129,138]

Clinical evidence revealed that SARS-CoV-2 infections predispose patients to subsequent bacterial or other viral infections, which are associated with poor outcomes including increased severity and fatality.[139,140] Based on what is known about the role of 3C^pro during picornaviral infections, at least two mechanisms may contribute to the secondary infections. First, TRIF is not only involved in antiviral but also participates in antibacterial host defense mechanisms.[141] Disruption of TRIF during the initial phase of viral infection could render the host more susceptible to bacterial invasions. Second, recent studies identified G3BP1 as a critical component in cyclic GMP-AMP synthase (cGAS)-mediated innate immune responses

against DNA viruses.[142,143] cGAS is a cytosolic DNA sensor that detects viral DNA to activate the IFN-I pathway.[144] Cleavage of G3BP1 is thus expected to weaken this mechanism and leave the patients at higher risk from a secondary DNA viral infection. A proposed model that picornaviruses (probably CoVs as well) induce two phases of infection (or co-infection) and disease progression is depicted in Figure 3.

2.2 | Targeting NLR family PYD containing protein-3 inflammasome pathway

Similar to RLRs, NLRs are cytosolic PRRs that sense intracellular PAMPs and/or danger-associated molecular patterns (DAMPs) to induce pro-inflammatory cytokine production and inflammatory cell death (termed pyroptosis).[145] Under stress, NLRs initiate the formation of a large multiprotein complex, called inflammasome. The best-studied inflammasome is the NLR family PYD containing protein-3 (NLRP3) inflammasome, which consists of the sensor NLRP3, the adapter apoptosis-associated speck-like protein containing a caspase recruitment domain (ASC), and the effector caspase-1. Upon sensing viral PAMPs and DAMPs generated during infection, NLRP3 oligomerizes and recruits pro-caspase-1 through the adapter protein ASC to form NLRP3 inflammasome. Subsequently, pro-caspase-1 undergoes self-cleavage and activation, promoting maturation and secretion of pro-inflammatory cytokine interleukin-1β (IL-1β) and IL-18, and inducing cleavage of the pro-pyroptotic factor gasdermin D (GSDMD).[146] The resulting N-terminal cleavage product of GSDMD then creates pores on cell membrane, triggering pyroptotic cell death and facilitating release of inflammatory cytokines (IL-1β and IL-18).[147] Similar to other types of cell death, pyroptosis limits viral replication by eliminating infected cells.

As NLRP3 plays a vital role in antiviral response, numerous viruses, including picornaviruses, have adopted strategies to counteract its functions.[145] It was reported that NLRP3-, ASC-, and caspase-1-deficient mice infected with EV-A71 display more severe disease phenotype and higher virus titers as compared to wild-type control mice, suggesting a defensive role for the NLRP3 inflammasome against EV-A71 infection.[52] Further investigation identified that, to overcome the antiviral immune response, EV-A71 has evolved to inactivate the NLRP3 inflammasome by directly cleaving NLRP3 through the proteolytic activities of 2A^pro and 3C^pro[52] In addition, EV-A71 3C^pro also targets its effector GSDMD for cleavage at a site (Gln193-Gly194) different from that (Asp275-Asp276) mediated by caspase-1. The cleavage products of GSDMD by 3C^pro fail to stimulate pyroptosis; hence, further enhancing EV-A71 replication. Similarly, following CVB3 infection, NLRP3^-/- mice present more rapid disease progression and increased viral loads when compared with wild-type mice. To evade the host defense, CVB3 3C^pro directly targets NLRP3 and its upstream signaling molecules (RIP1/RIP3, receptor-interacting protein 1/3) for degradation.[53,62,148]
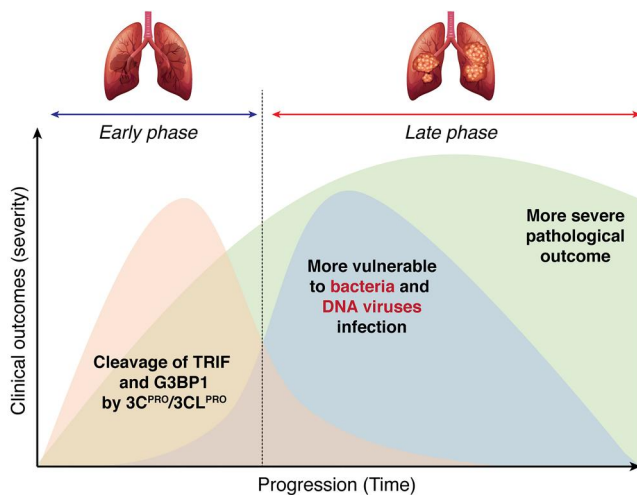
FIGURE 3 A proposed mechanistic model for the secondary infection after the initial picornavirus or coronavirus infection. During the first phase of infection, proteins (e.g., TRIP and G3BP1) that are involved in a broad range of host defenses (i.e., against not only RNA viral infection, but also bacterial and DNA viral invasion) are targeted by 3C protease or possibly 3C-like protease for degradation, rendering the patients more vulnerable to secondary infection. Combinatorial infection during the late phase could result in increased disease severity and mortality

It is increasingly recognized that early, temporary activation of NLRP3 inflammation has an antiviral role by clearing virus and infected cells, whereas prolonged and extreme activation is harmful, causing disease-related immunopathology. For example, during hepatitis C viral infection, activation of NLRP3 inflammasome is associated with enhanced inflammation and tissue damage.[149] Persistent activation of NLRP3 during CVB3 infection has also been linked to pathological outcome.[150,151] It is well documented that SARS-CoV-2 infection leads to cytokine storm, featured by excessive production and secretion of pro-inflammatory cytokines and chemokines, contributing significantly to disease severity of Covid-19.[5,122,152] Several proteins encoded by SARS-CoV, including E, ORF3a, and ORF8b, have been shown to activate the NLRP3 inflammasome.[153–155] Recent evidence has also revealed that NLRP3 inflammasome is activated in response to SARS-CoV-2 infection.[156] It is speculated that overactivation of the inflammasome may be responsible, at least in part, for the observed cytokine storm in Covid-19 patients.

The NLRP inflammasome pathway and viral manipulation are summarized in Figure 4.

2.3 | Targeting host RNA degradation components

In eukaryotic cells, posttranscriptional processes (e.g., mRNA surveillance, silencing, translational repression, and degradation) play a central role in the regulation of gene expression and ultimately determine the expression levels of a significant fraction of the transcriptome. Recently, it has become apparent that posttranscriptional processes acting on cytoplasmic messenger ribonucleoprotein complexes (mRNPs) are physically tied and can occur in discrete cytoplasmic entity known as processing (P)-bodies. These compartments are highly conserved across cells derived from vertebrates, invertebrates, yeasts and plants, containing many enzymes involved in mRNA turnover. To date, P-bodies have been demonstrated to play critical roles in general mRNA degradation, nonsense-mediated
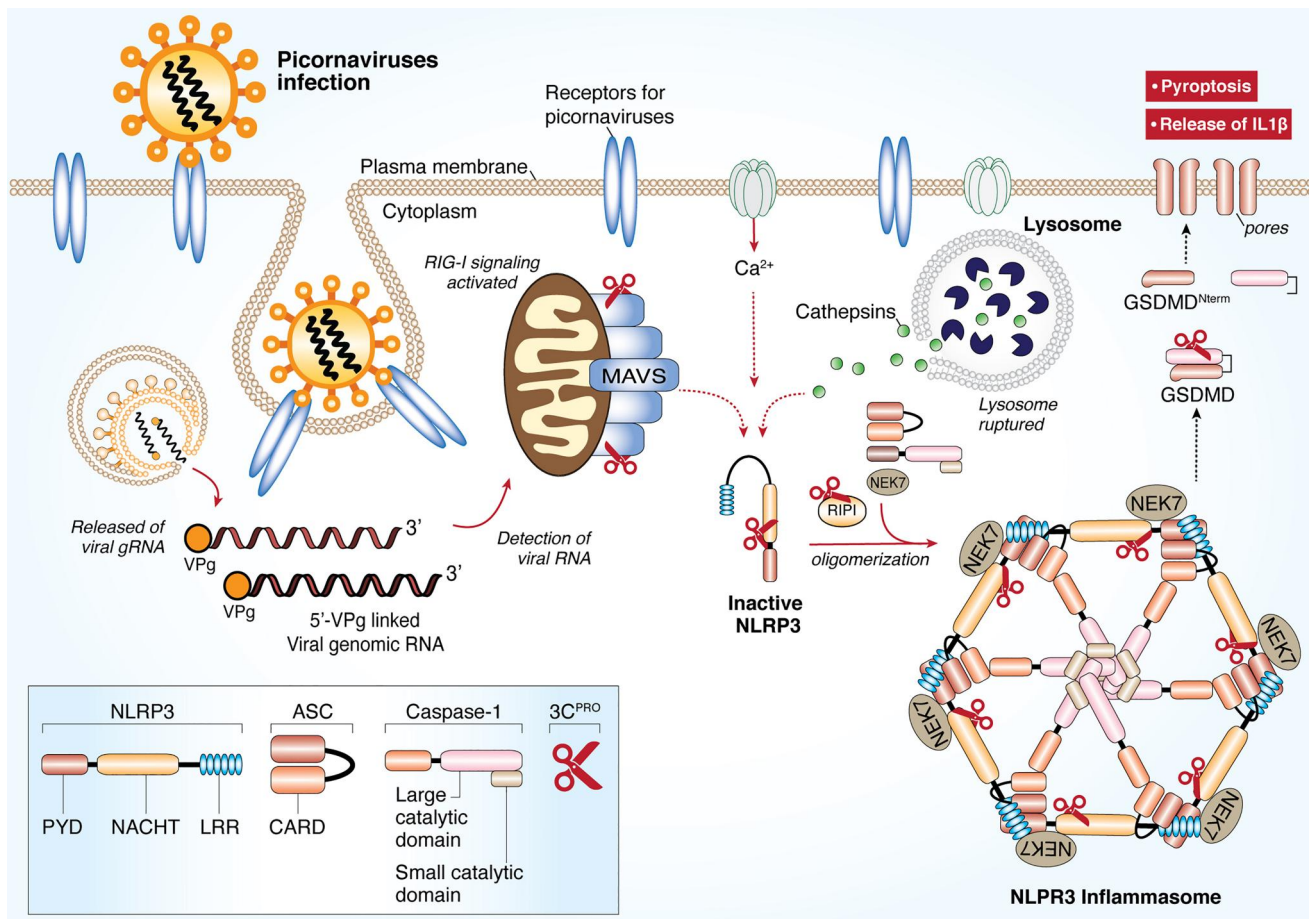
FIGURE 4 Picornaviral 3C[pro] targets the NLRP3 inflammasome for immune evasion. RNA viruses and other DAMPs could activate NLRP3 inflammasome. Formation of the NLRP3-dependent inflammasome activates caspase 1, which in turn cleaves pro-IL-1β and pro-IL-18. GSDMD is also cleaved by caspase 1 and the resulting N-terminal cleavage products are inserted into the plasma membrane, forming multiple pores and inducing pyroptosis and release of pro-inflammatory cytokine. Upon picornaviral infection, NLRP3, its upstream signaling proteins (RIP1/RIP3), and its downstream effector GSDMD are all targeted by 3C[pro] for degradation. As a result, pyroptosis is inhibited for efficient viral replication. CARD, caspase activation and recruitment domain; DAMPs, danger-associated molecular patterns; GSDMD, Gasdermin D; LRR, Leucine rich repeat; NLRP3, NLR family and pyrin domain-containing protein 3; PYD, Pyrin domain; RIP, receptor-interacting protein; NACHT, NAIP, CIITA, HET-E and TEP1-associated families; VPg, viral protein genome-linked; 3C[pro], 3C protease

mRNA decay, adenylate-uridylate-rich (AU-rich) element-mediated mRNA degradation at the 3′ UTRs, and miRNA-induced RNA silencing pathway.[157]

In eukaryotes, the degradation process is initiated firstly by removal of the poly(A) tail by deadenylases. Following deadenylation, mRNAs are subjected to exonucleolytically degradation starting from their 3′-end by the exosome, a multimeric complex with 3′→5′ exonucleases. In the meantime, the guanosine cap structure at the 5′-end is removed by several decapping enzymes and coactivators, including decapping protein 1/2 (DCP1/2), DEAD-box RNA-helicase-6 (DDX6), enhancer of mRNA decapping protein-3 (EDC3) and EDC4, rendering the mRNA susceptible to 5′→3′ degradation by the major cytoplasmic exoribonuclease 1 (XRN1).[158]

RNA degradation has emerged as an important antiviral host defense mechanism.[158] The most widely studied viruses in the context of XRN1 are positive-stranded RNA viruses from the *Flaviviridae* family, including Dengue virus, West Nile viruses, hepatitis C
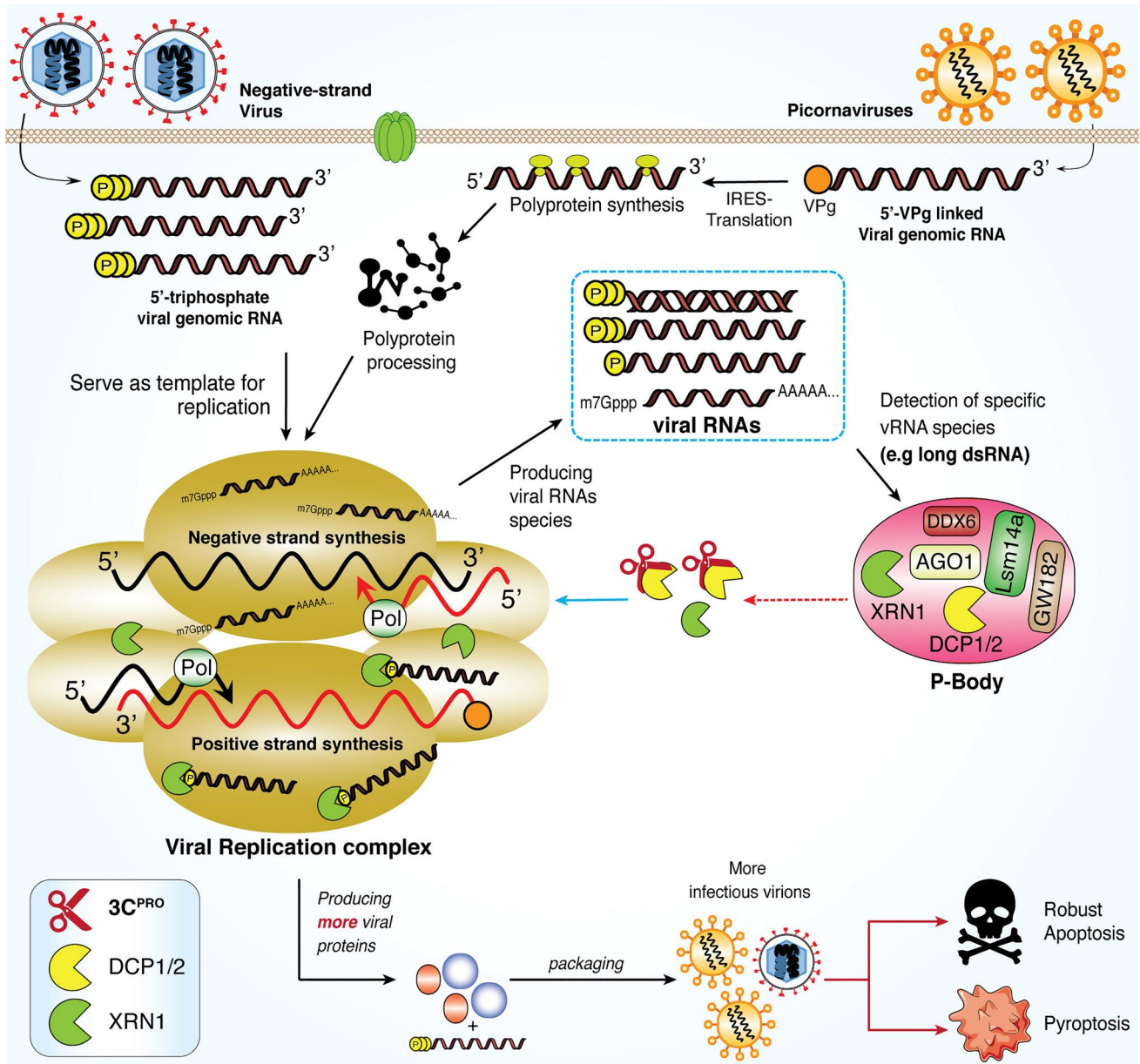
FIGURE 5 Dispersion of 5′→3′ RNA degradation components within P-bodies during picornaviral infection. RNA viruses, including picornaviruses, initiate viral replication in a discrete compartment within cytoplasm, generating various RNA species with defined signatures. These includes 5′ppp, 5′p-ssRNA, dsRNA and viral mRNA. Both picornavirus and coronavirus are able to generate long ssRNA and dsRNA and trigger the translocation of 5′→3′ RNA degradation components, including DCP1, DCP2, and XRN1, into the viral replication complex for degradation of associated viral RNA species. Picornaviral 3C^pro cleaves DCP1, resulting in increased viral particles and infectivity. DCP1/2, decapping protein-1/2; XRN1, 5′→3′ exoribonuclease-1; dsRNA, double-stranded RNA; 3C^pro, 3C protease

virus, and Yellow Fever virus. XRN1 acts as an antiviral factor by degrading their genomic RNA.[157] In addition, DCP1/2-XRN1 were shown to have critical antiviral functions against both picornaviruses and negative-stranded cytoplasmic RNA viruses. During infection, these viruses generate various RNA intermediate species with defined structures (long/short dsRNA and ssRNA) inside their replication complexes. Both long ssRNA and dsRNA could induce the re-localization of both DCP1/2 and XRN1 nucleases into the viral replication complexes for viral RNA degradation.[159] This further supports the prior observation that the presence of XRN1 and DCPs potentially poses a threat to enterovirus RNA. To conquer this antiviral activity, PV utilizes its 3C^pro to disperse and destabilize P-bodies by directly targeting DCP1a for degradation.[103] The interplay between the cellular RNA degradation pathway and the viruses is illustrated in Figure 5.

While both the genomic and subgenomic SARS-CoV-2 mRNAs contain 5′-cap structure, previous studies have shown that inhibiting several eukaryotic initiation factors family proteins (eIF4E, eIF4F, and eIF4G) could impair coronavirus replication,[160,161] highlighting

the importance of cap-dependent translation in SARS-CoV-2 mRNA synthesis. Thus, it is not surprising that SARS-CoV-2 would intervene the function of host decapping enzyme DCP1/2 and XRN1, possibly through its 3CL^pro. However, to date, antiviral roles XRN1 in coronaviral mRNA translation have not been reported.

2.4 | Targeting host autophagy machinery

Macroautophagy (or autophagy in short) is a conserved intracellular degradation pathway that is essential in maintaining cellular homeostasis by removing unwanted or dysfunctional cellular components.[162] The process of autophagy is highly regulated by more than 30 "autophagy-related" proteins and includes three major steps. First, the substrates are sequestered by a crescent-shaped double-membrane vesicle called a phagophore. Then, the two ends of the phagophore fuse to form an autophagosome. Finally, autophagosome fuses with a lysosome while the enwrapped cargo is degraded by hydrolysis.
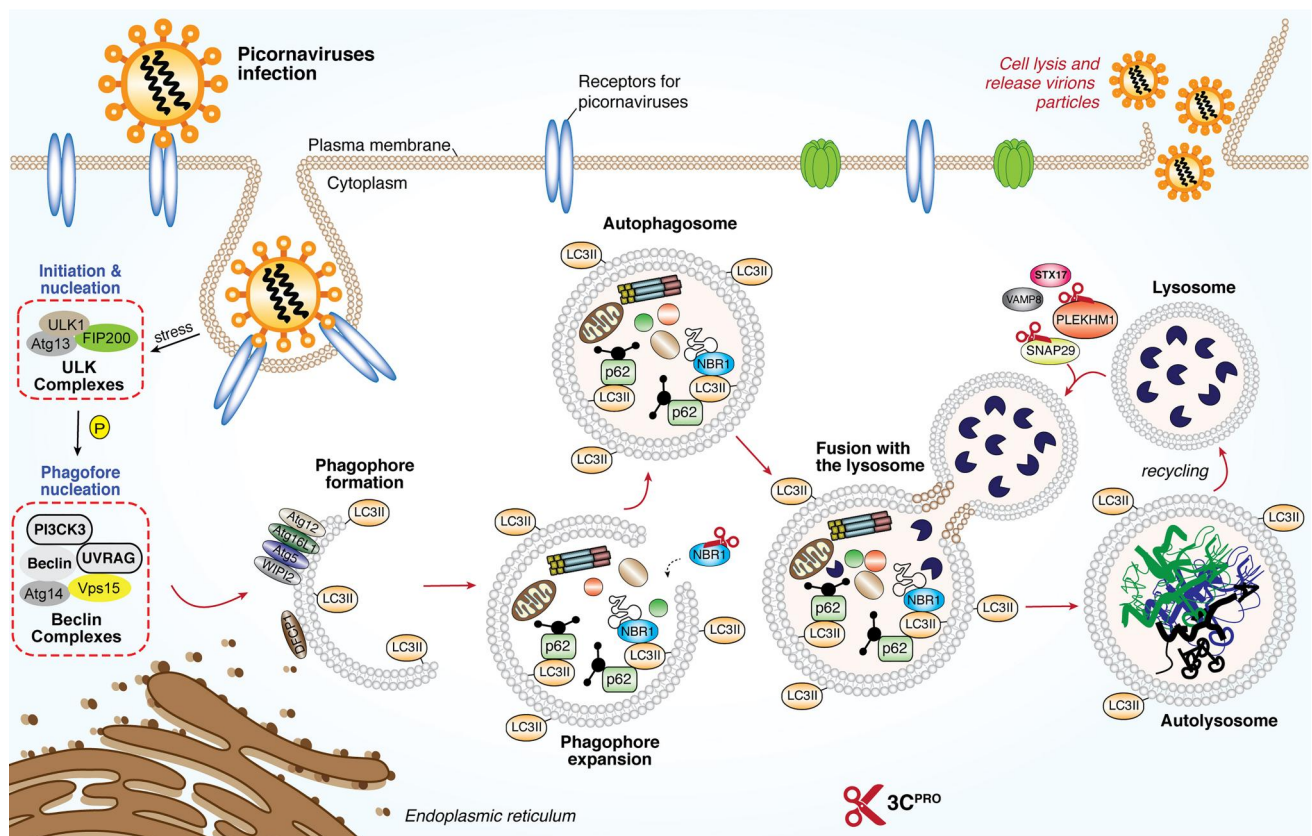
FIGURE 6 Subversion of host autophagy through picornaviral 3C^pro. Schematic diagram depicted the molecular mechanism for the initiation of host autophagy pathway upon the presence of RNA virus for the clearance of viral-associated molecules. Picornaviruses utilize its own encoded 2A^pro (not shown here) and 3C^pro to cleave key components such as p62, NBR1, SNAP29 and PLEKHM1 to facilitate a more robust replication. ATGs, autophagy-related genes; DFCP1, double FYVE-containing protein-1, FIP200, focal adhesion kinase family interacting protein of 200kD; NBR1, neighbor of BRCA1; SNAP29, synaptosomal-associated protein-29; PLEKHM1, Pleckstrin homology and RUN domain containing M1; p62, also known as sequestosome 1 (SQSTM1); STX17, Syntaxin 17; ULK, Unc-51-like kinase-1; UVRAG, UV radiation resistance-associated gene protein; VAMP8, vesicle-associated membrane protein-8; WIPI2, WD-repeat domain phosphoinositide-interacting protein-2; 2A^pro, 2A-protease; 3C^pro, 3C protease

Autophagy plays a significant role in antiviral host defense by directly targeting invading viruses through a process, call virophagy, for clearance.[163,164] Virophagy is mediated through the function of autophagy cargo receptors, including sequestosome 1 (SQSTM1)/p62, neighbor of *BRCA1* (NBR1), calcium binding and coiled-coil domain-containing protein 2 (CALCOCO2)/nuclear dot 10 protein 52 (NDP52), which recruit viral components/particles to autophagosome for degradation.[165] To evade the antiviral efforts of virophagy, many viruses, including picornaviruses, have evolved to disrupt the function of autophagy receptors.[166] For instance, SQSTM1/p62 and CALCOCO2/NDP52 are targeted for degradation by CVB3 2A^{pro} and 3C^{pro}, respectively.[66,67] Cleavage of SQSTM1/p62 was later confirmed upon PV, HRV-1A, and EV-D68 infection.[68] Furthermore, NBR1, a homolog of SQSTM1/p62, can

also be cleaved by 3C^{pro}[69]. Remarkably, it was found that cleavage of SQSTM1/p62 and NBR1 not only causes a loss-of-function, but also generates dominant-negative mutants against the function of native proteins.[69] Loss of both SQSTM1/p62 and NBR1 would also impair mitophagy and results in mass production of reactive oxygen species, and IL-1β through constitutive NLRP3-independent inflammasome activation (potentially other NLRP family members).[167] The resulting cleavage fragments of SQSTM1/p62 and NBR1 will accumulate to serve as DAMPs signals and further amplify the inflammatory cascade. Acute respiratory pneumonia due to cytokine storm is a hall mark of SARS-CoV-2 infection, whether its 3CL^{pro} would manipulate host autophagic system in particular to mass produced IL-1β in Covid-19 pathogenesis is certainly worth further investigation.
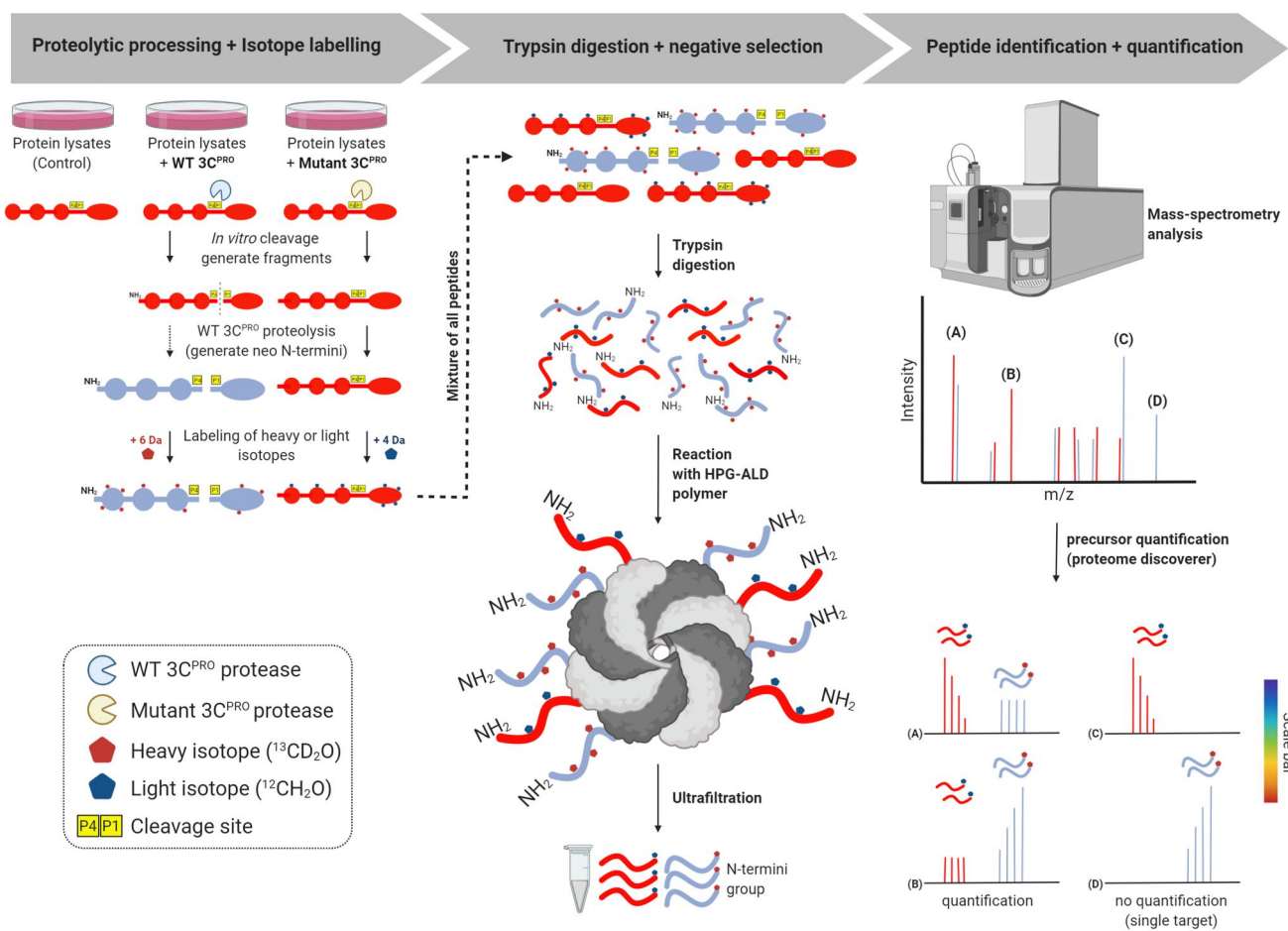
FIGURE 7 Schematic workflow of TAILS N-terminomics screening of 3C^{pro} and 3CL^{pro} substrates. Schematic diagram depicts the TAILS workflow and scheme for identification of 3C^{pro} or 3CL^{pro} substrates. In brief, protein samples from whole cell lysates were subjected to in vitro cleavage by either recombinant purified WT 3C^{pro}/3CL^{pro} or mutant (C147A) 3C^{pro}/(C145A) 3CL^{pro}, followed by N-terminal enrichment using TAILS (*left panel*). Samples were then combined and subjected to pre-TAILS shotgun-like mass-spectrometry analysis after complete digestion with trypsin. The exposed amine groups of N-termini generated by the trypsin digestion were then removed by covalently coupling to a high-molecular weight polyaldehyde polyglycerol polymer. This process allowed for selection via negative enrichment of blocked N termini (*middle panel*). Peptides were subsequently identified and quantified using high-resolution mass spectrometry (indicated in the *right panel*). The resultant high-confidence candidate substrates were determined through the analysis of the quantified heavy/light (H/L) ratio of dimethylation-labeled semitryptic neo-N terminus peptides. They will be subjected to further validation through similar in vitro cleavage assay by 3C^{pro}/3CL^{pro}, followed by immunoblotting using specific antibodies; TAILS, terminal amine isotopic labeling of substrates; 3C^{pro}, 3C protease; 3CL^{pro}, 3C-like protease

TABLE 2 Studies of 3C^{pro} or 3CL^{pro} inhibitors antiviral compounds [Correction added on 17 February 2021, after first online publication. The references were updated throughout Table 2 and in-text citations.]

Research phase	Compound	Target	Results	Ref
In vitro validation	TG-0205221	3CL^{pro} of SARS-CoV and HCoV-229E	Reduces SARS-CoV and HCoV-229E replication by titer of 4.7 Log$_{10}$	[191]
	Flavonoids: Apigenin, luteolin, quercetin, amentoflavone, aueretin, daidzein, puerarin, epigallocatechin gallate, gallocatechin gallate, kaempferol,rhoifolin, pectolinarin, herbacetin, flavonol	SARS-CoV 3CL^{pro}	Inhibit SARS-CoV 3CL^{pro} FRET protease assay catalytic activity	[192]
	Pyrazolone and pyrimidines inhibitors	SARS-CoV 3CL^{pro}	Show potent inhibitory activities against SARS-CoV 3CL^{pro} at micromolar range.	[193]
	Aryl methylene ketones, Mono-, and difluorinated methylene ketones groups	SARS-CoV 3CL^{pro}	Improved version is stable and less toxic to cells. Potently inhibits SARS-CoV 3CL^{pro} at nanomolar range	[194]
	Heteroaromatic esters and benzotriazole esters derivatives	SARS-CoV 3CL^{pro}	Show potent inhibitory activities against SARS-CoV 3CL^{pro} at nanomolar range	[195–197]
	Boronic	SARS-CoV 3CL^{pro}	Significantly inhibits SARS-CoV 3CL^{pro} enzymatic activity in micromolar range	[198]
	Aza-peptide epoxides derivatives	SARS-CoV 3CL^{pro}	Show irreversible inhibition against SARS-CoV 3CL^{pro}	[199–201]
	Etacrynic acid derivatives	SARS-CoV PL^{pro} and 3CL^{pro}	Show more than 70% inhibition on SARS-CoV at concentration of 100μM	[202,203]
	Peptides aldehydes derivatives	SARS-CoV and HCoV-229E 3CL^{pro}	Suppress SARS-CoV by 4.7 Log$_{10}$ and HCoV-229E by 5.2 Log$_{10}$	[191]
	Modified version of HIV protease inhibitors	SARS-CoV 3CL^{pro}	Potent inhibitors against SARS-CoV 3CL^{pro} but not against HIV protease	[204]
	Sulfone and dihydroimidazole derivatives	SARS-CoV 3CL^{pro}	21 derivatives from these two analogs show EC$_{50}$ less than 50 μM against SARS-CoV 3CL^{pro}	[205,206]
	Michael acceptor peptidomimetics	SARS-CoV 3CL^{pro}	Show potent inhibitory against SARS-CoV 3CL^{pro}	[207,208]
	Lignoids, di- and triterpenoid derivatives: Betulinic acid, savinin, ferruginol, pritimererin, tingenone, iguestrin and triterpenoids celastrol	SARS-CoV 3CL^{pro}	Abietane type diterpenoids are the most robust terpenoids on SARS-CoV (EC$_{50}$ = 9.1 μM)	[209–211]
	Metal conjugated: Zinc- or mercuric based	SARS-CoV PLpro and 3CL^{pro},	Inhibition is pronounced in Zinc-conjugated compounds	[212,213]
	α-Ketoamides:	3C^{pro} of CVB3, &; HRV, EV-D68, EV-A713CL^{pro} of SARS-CoV, MERS, 229E	Display low toxicity &; low micromolar of EC$_{50}$ against tested viruses	[214]
	Pyridyl, pyrazyl and Benzotriazole-derivatives inhibitors	SARS-CoV PL^{pro} or 3CL^{pro}	Robust inhibition on SARS-CoV in vitro within micromolar range	[215–217]
	Rupintrivir (AG-7088)	Targeting 3C^{pro} and 3CL^{pro} encoding viruses	Shows robust activity against SARS-CoV-2 in vitro	[218,219]
	Boceprevir, Calpain inhibitors II, and XII	SARS-CoV-2 3CL^{pro}	Inhibit SARS-CoV-2 in vitro with EC$_{50}$ less than 5μM	[220]
	3CL^{pro}-1	Originally designed for 3C^{pro} of EV-A71.	Shows robust efficacy of EC$_{50}$ 200 nM, effective against SARS-CoV-2 and MERS-CoV.	[221,222]
	Isatin derivatives	Targeting 3C^{pro} and SARS-CoV 3CL^{pro}	Effectively inhibit SARS-CoV 3CL^{pro} through noncovalent bonding in low micromolar range	[223,224]
	Anilide derivaties: 2-chloro-4-nitro anilineL-phenylalanine, 4-(dimethylamino)benzoic acid	SARS-CoV 3CL^{pro}	Potent and highly specific inhibitors against SARS-CoV 3CL^{pro}	[225]

TABLE 2 (Continued)

Research phase	Compound	Target	Results	Ref
Computational prediction (docking analysis)	**Anti-HIV-1 drugs**: Indinavir, Darunavir	SARS-CoV-2 3CL^{pro}	Docking & binding free energy prediction shows high scores & high binding affinities against SARS-CoV-2 3CL^{pro}	226
	Decahydroisoquinoline inhibitors	SARS-CoV-2 3CL^{pro}	X-ray crystallization studies confirmed that these inhibitors fit well into the cleft of 3CL^{pro}	227
In vitro and *in vivo* validation	Peptides with halomethyl ketone derivatives	SARS-CoV 3CL^{pro}	Effectively inhibit SARS-CoV infection, with low cytotoxicity in cells and in mice.	228
Widely tested in animals and now under trial on human for coronavirus disease-2019	GC376	Targeting 3C^{pro} and 3CL^{pro} encoding viruses	Shows robust activity against SARS-CoV, SARS-CoV-2, and Norovirus	220

Abbreviations: HRV, human rhinovirus; MERS-CoV, Middle East respiratory syndrome-CoV; PLpro, papain-like protease; SARS-CoV-2, severe acute respiratory syndrome coronavirus-2 3CL^{pro}/3C^{pro}, 3C-like protease/3C protease.

Decreased autophagic flux as a result of blockage of autophagosome-lysosome fusion is another mechanism adopted by picornaviruses to escape viral RNA/protein degradation. The fusion process is regulated by multiple proteins involved in membrane trafficking, particularly a group of SNAP29 proteins, including syntaxin 17 (STX17), synaptosomal-associated protein 29 (SNAP29), and vesicle-associated membrane protein 8 (VAMP8).[168] It was discovered that upon EV-D68 and CVB3 infection, the SNAP29 linker protein, SNAP29, is cleaved by 3C^{pro}, which dissociates the STX17-interacting domain of SNAP29 from the VAMP8-binding motif, thereby disrupting the formation of STX17-SNAP29-VAMP8 complexes and inhibiting autophagosome-lysosome fusion.[68,70] Figure 6 summarizes the known mechanism by which picornaviral protease subverts the autophagy for immune evasion.

Similar to the observations made with several picornaviruses, it was recently demonstrated that SARS-CoV-2 infection impairs autophagic flux by blocking autophagosome fusion with a lysosome and induction of autophagy reduces viral replication.[169] This finding is consistent with an earlier report with MERS-CoV infection by the same research group.[170] Although the mechanism responsible for decreased autophagosome-lysosome fusion remains largely unclear, it was previously shown that over-expression of the membrane-associated PL^{pro} of SARS-CoV and MERS-CoV is sufficient to suppress the fusion between autophagosome and lysosome,[171] whether CoV 3CL^{pro} has a role in regulation of autophagic flux and cargo recognition in general as some picornaviral 3C^{pro} does has not been explored and requires further investigations. The list of substrates of 3C^{pro} and 3CL^{pro} is summarized in Table 1.

2.5 | High-throughput identification of cellular substrates of 3C^{pro}

A proteomics-based quantitative method, termed N-terminomic terminal amine isotopic labeling of substrates (TAILS) (Figure 7),[172]

has been exploited to globally search for novel cellular substrates of picornaviral proteases.[63,85] TAILS, developed by the Overall laboratory at the University of British Columbia, uses an unbiased negative selection approach to identify neo-N and -C termini (named N-terminomic and C-terminomic TAILS, respectively).[172–175] This state-of-the-art approach has several advantages, including quantitative, highly sensitive, and concurrent identification of both the substrates and the cleavage sites,[176] and has been used to analyze substrates of many types of proteases.[177,178]

Jan and colleagues conducted N-terminomic TAILS on HeLa cell or mouse cardiomyocyte extracts subjected to incubation with purified recombinant PV or CVB3 3C^{pro}, respectively, to identify cleaved neo-N-terminal peptides (see Figure 7 for the detailed procedure).[63,85] A list of high confidence candidate proteins was generated for 3C^{pro}, including peptides corresponding to previously reported substrates at the known cleavage sites (i.e., poly(A) binding protein (PABP),[90] G3BP1[110] and TAR DNA-binding protein 43 (TDP-43)[87]). Among them, a subset of candidate targets of PV 3C^{pro} has been validated in vitro and under viral infection, which include four common protein substrates of both PV and CVB3 3C^{pro} (i.e., heterogeneous nuclear ribonucleoprotein M (hnRNP M), hnRNP K, RIP1, and phosphoribosylformylglycinamidine synthetase [PFAS]), programmed cell death 6-interacting protein (PDCD6IP, also known as ALIX), general vesicular transport factor p115, ATP-citrate synthase (ACLY), Golgi-specific brefeldin A-resistance guanine nucleotide exchange factor 1 (GBF1). Studies through gene-silencing or expression of a non-cleavable mutant form of these substrates have demonstrated a pivotal role for these proteins in regulating viral replication/propagation.[63,85]

Given the effectiveness of the N-terminomic TAILS in identifying the cellular targets of 3C^{pro}, this unbiased proteomics approach is currently being utilized to analyze the cellular targets of MHV and SARS-CoV-2 proteases, including 3CL^{pro}. It is anticipated that identification of the full repertoire of host substrates of CoV proteases will provide a more comprehensive understanding of viral tropism,

interaction with host cells, and pathogenesis, as well as assist in the development of novel antiviral drugs.

2.6 | Current 3C^{pro} and 3CL^{pro} inhibitors and future challenges

As discussed earlier, both picornaviral 3C^{pro} and coronaviral 3CL^{pro} are chymotrypsin-like cysteine proteases with conserved substrate specificity (P1-P1′ and P4 cleavage sites of the substrates are highly conserved between two enzymes) and active sites.[179] Owing to these similarities, efforts have been made to explore the potential of developing broad-spectrum antiviral compounds.[13–15] The fact that no known human homologs further increases the feasibility of this strategy.

Rupintrivir (AG-7088, a protease inhibitor originally developed for HRV to treat common cold) and/or its derivatives/analogs have been found to possess antiviral activities against a wide range of picornaviruses (i.e., HRV, PV, EV-A71, EV-D68, CVB, CVA, HAV, and FMDV)[180–183] and coronaviruses, including SARS-CoV.[14,184] Furthermore, it was reported that dipeptidyl aldehyde (GC373), α-ketoamide (GC375), and dipeptidyl bisulfite adduct (GC376), are able to inhibit both picornaviral 3C^{pro} and coronaviral 3CL^{pro} activities and block viral replication.[13] These studies point to the possibility of developing broad-spectrum antiviral therapeutics against SARS-CoV-2. However, rupintrivir failed to show efficacy in natural HRV infection conditions during a clinical phase II trial.[185]

Although Remdesivir (a nucleotide analog inhibitor of RdRp, originally developed for the treatment of Ebola virus disease by Gilead Sciences) has been approved for treating severely ill Covid-19 patients in the United States and the Europe,[186] its safety and antiviral activity are still under extensive investigations and clinical trials. Similarly, despite some early promising findings showing the effectiveness of chloroquine (a classical anti-malarial and autoimmune disease drugs) against SARS-CoV-2 infection in non-respiratory cells,[187,188] recent research has demonstrated that chloroquine fails to block infection of human lung epithelial cells with SARS-CoV-2.[189] In addition, it is known that chloroquine may cause severe cardiotoxicity.[190] A number of attempts have been made to design drugs targeting 3CL^{pro} of SARS-CoV-2. Different approaches, including laboratory synthesis, virtual screening, drug repositioning, and structure-based molecular docking have been taken for this purpose. Hilgenfeld laboratory recently elucidated the X-ray crystallographic structure of SARS-CoV-2 3CL^{pro} and synthesized improved α-ketoamide inhibitors to target 3CL.[12] Using computer-aided drug design, Jin et al. identified a 3CL^{pro} inhibitor (N3) and determined the crystal structure of its complex with 3CL^{pro} of SARS-CoV-2[10]. Through a combined structure-based virtual and high-throughput screening, they further showed that six compounds exhibit potent anti-3CL^{pro} activities.[10] Most recently, Dai et al. reported the design and synthesis of two lead compounds (11a and 11b) targeting 3CL^{pro} and solved the X-ray crystal structure of these inhibitors bound to 3CL.[9] Although these compounds serve as promising drug candidates, their effectiveness in nature infection remain to be investigated. The list of inhibitors targeting 3C^{pro} and 3CL^{pro} is summarized in Table 2.

3 | CONCLUDING REMARKS

To date, we know very little about the 3CL^{pro} of SARS-CoV-2, especially the molecular mechanism of the pathways by which SARS-CoV-2 3CL^{pro} blocks. Certainly, we cannot rule out that there are some differences but also a lot of similarities among both families. While we are in the process of understanding the structure and functions of SARS-CoV-2 3CL^{pro}, a comparison with the 3C^{pro} from picornaviruses can provide more insights into the pathogenesis and regulatory mechanisms of Covid-19. These will serve as a critical foundation for the design of broad-spectrum anti-coronaviruses inhibitors, or perhaps anti-3C/3CL^{pro} expressing viruses.

CONFLICT OF INTEREST
The authors declare that they have no conflict of interest.

AUTHORS CONTRIBUTIONS
Chen Seng Ng and Honglin Luo designed and outlined the review. Chen Seng Ng prepared the initial manuscript and figures. Christopher C. Stobart prepared the structural figure and relevant information. All authors contributed to revising and writing the final version.

DATA AVAILABILITY STATEMENT
Data sharing not applicable to this article as no datasets were generated or analyzed during the current study.

ORCID
Honglin Luo https://orcid.org/0000-0002-7708-7840

REFERENCES
1. Zhou P, Yang X-L, Wang X-G, et al. A pneumonia outbreak associated with a new coronavirus of probable bat origin. *Nature.* 2020;579:270-273.
2. Zhu N, Zhang D, Wang W, et al. A novel coronavirus from patients with pneumonia in China, 2019. *N Engl J Med.* 2020;382:727-733.

3. Coronaviridae Study Group of the International Committee on Taxonomy of Viruses. The species Severe acute respiratory syndrome-related coronavirus: classifying 2019-nCoV and naming it SARS-CoV-2. *Nat Microbiol.* 2020;5:536-544.

4. Wadman M, Couzin-Frankel J, Kaiser J, Matacic C. A rampage through the body. *Science.* 2020;368:356-360.

5. Huang C, Wang Y, Li X, et al. clinical features of patients infected with 2019 novel coronavirus in Wuhan, China. *Lancet.* 2020;395:497-506.

6. Wu Z, McGoogan JM. Characteristics of and important lessons from the coronavirus disease 2019 (COVID-19) outbreak in China: summary of a report of 72 314 cases from the Chinese center for disease control and prevention. *J Am Med Assoc.* 2020; 323(13):1239–1242. https://doi.org/10.1001/jama.2020.2648.

7. Saberi A, Gulyaeva AA, Brubacher JL, Newmark PA, Gorbalenya AE. A planarian nidovirus expands the limits of RNA genome size. *PLoS Pathog.* 2018;14:e1007314.

8. Gordon DE, Jang GM, Bouhaddou M, et al. A SARS-CoV-2 protein interaction map reveals targets for drug repurposing. *Nature.* 2020;583:459-468.

9. Dai W, Zhang B, Jiang X-M, et al. Structure-based design of antiviral drug candidates targeting the SARS-CoV-2 main protease. *Science.* 2020;368:1331-1335.

10. Jin Z, Du X, Xu Y, et al. Structure of Mpro from SARS-CoV-2 and discovery of its inhibitors. *Nature.* 2020;582:289-293.

11. Anand K, Ziebuhr J, Wadhwani P, Mesters JR, Hilgenfeld R. Coronavirus main proteinase (3CLpro) structure: basis for design of anti-SARS drugs. *Science.* 2003;300:1763-1767.

12. Zhang L, Lin D, Sun X, et al. Crystal structure of SARS-CoV-2 main protease provides a basis for design of improved α-ketoamide inhibitors. *Science.* 2020;368:409-412.

13. Kim Y, Lovell S, Tiew K-C, et al. Broad-spectrum antivirals against 3C or 3C-like proteases of picornaviruses, noroviruses, and coronaviruses. *J Virol.* 2012;86:11754-11762.

14. Kuo C-J, Liu H-G, Lo Y-K, et al. Individual and common inhibitors of coronavirus and picornavirus main proteases. *FEBS Lett.* 2009;583:549-555.

15. Ramajayam R, Tan K-P, Liang P-H. Recent development of 3C and 3CL protease inhibitors for anti-coronavirus and anti-picornavirus drug discovery. *Biochem Soc Trans.* 2011;39:1371-1375.

16. Lefkowitz EJ, Dempsey DM, Hendrickson RC, et al. Virus taxonomy: the database of the international committee on taxonomy of viruses (ICTV). *Nucleic Acids Res.* 2018;46:D708-D717.

17. Sun D, Chen S, Cheng A, Wang M. Roles of the picornaviral 3C proteinase in the viral life cycle and host cells. *Viruses.* 2016;8:82.

18. Wang Y, Ma L, Stipkovits L, Szathmary S, Li X, Liu Y. The strategy of picornavirus evading host antiviral responses: non-structural proteins suppress the production of IFNs. *Front Microbiol.* 2018;9:2943.

19. Wang J, Fan T, Yao X, et al. Crystal structures of enterovirus 71 3C protease complexed with rupintrivir reveal the roles of catalytically important residues. *J Virol.* 2011;85:10021-10030.

20. Hämmerle T, Hellen CU, Wimmer E. Site-directed mutagenesis of the putative catalytic triad of poliovirus 3C proteinase. *J Biol Chem.* 1991;266:5412-5416.

21. Zunszain PA, Knox SR, Sweeney TR, et al. Insights into cleavage specificity from the crystal structure of foot-and-mouth disease virus 3C protease complexed with a peptide substrate. *J Mol Biol.* 2010;395:375-389.

22. Ypma-Wong MF, Dewalt PG, Johnson VH, Lamb JG, Semler BL. Protein 3CD is the major poliovirus proteinase responsible for cleavage of the P1 capsid precursor. *Virology.* 1988;166:265-270.

23. Chan YM, Boehr DD. Allosteric functional switch in poliovirus 3C protease. *Biophys J.* 2015;108:528a.

24. Roehl HH, Parsley TB, Ho TV, Semler BL. Processing of a cellular polypeptide by 3CD proteinase is required for poliovirus ribonucleoprotein complex formation. *J Virol.* 1997;71:578-585.

25. Anand K, Palm GJ, Mesters JR, Siddell SG, Ziebuhr J, Hilgenfeld R, et al. Structure of coronavirus main proteinase reveals combination of a chymotrypsin fold with an extra alpha-helical domain. *Embo J.* 2002;21:3213-3224.

26. Gorbalenya AE, Donchenko AP, Blinov VM, Koonin EV. Cysteine proteases of positive strand RNA viruses and chymotrypsin-like serine proteases. A distinct protein superfamily with a common structural fold. *FEBS Lett.* 1989;243:103-114.

27. Lu Y, Denison MR. Determinants of mouse hepatitis virus 3C-like proteinase activity. *Virology.* 1997;230:335-342.

28. Tomar S, Johnston ML, St John SE, et al. Ligand-induced dimerization of Middle East respiratory syndrome (MERS) coronavirus nsp5 protease (3CLpro): IMPLICATIONS for nsp5 regulation and the development OF antivirals. *J Biol Chem.* 2015;290:19403-19422.

29. Akira, S, Uematsu, S & Takeuchi, O Pathogen recognition and innate immunity. *Cell.* 2006;124:783–801.

30. Ng CS, Kato H, Fujita T. Fueling type I interferonopathies: regulation and function of type I interferon antiviral responses. *J Interferon Cytokine Res.* 2019;39:383-392.

31. Roth-Cross JK, Bender SJ, Weiss SR. Murine coronavirus mouse hepatitis virus is recognized by MDA5 and induces type I interferon in brain macrophages/microglia. *J Virol.* 2008;82:9829-9838.

32. Peisley A, Lin C, Wu B, et al. Cooperative assembly and dynamic disassembly of MDA5 filaments for viral dsRNA recognition. *Proc Natl Acad Sci USA.* 2011;108:21010-21015.

33. Barral PM, Sarkar D, Fisher PB, Racaniello VR. RIG-I is cleaved during picornavirus infection. *Virology.* 2009;391:171-176.

34. Drahos J, Racaniello VR. Cleavage of IPS-1 in cells infected with human rhinovirus. *J Virol.* 2009;83:11581-11587.

35. Lei X, Xiao X, Xue Q, Jin Q, He B, Wang J. Cleavage of interferon regulatory factor 7 by enterovirus 71 3C suppresses cellular responses. *J Virol.* 2013;87:1690-1698.

36. Mukherjee A, Morosky SA, Delorme-Axford E, et al. The coxsackievirus B 3C protease cleaves MAVS and TRIF to attenuate host type I interferon and apoptotic signaling. *PLoS Pathog.* 2011;7: e1001311.

37. Rui Y, Su J, Wang H, et al. Disruption of MDA5-mediated innate immune responses by the 3C proteins of coxsackievirus A16, coxsackievirus A6, and enterovirus D68. *J Virol.* 2017;91(13): e00546–17.

38. Yang Y, Liang Y, Qu L, et al. Disruption of innate immunity due to mitochondrial targeting of a picornaviral protease precursor. *Proc Natl Acad Sci USA.* 2007;104:7253-7258.

39. Wen W, Yin M, Zhang H, et al. Seneca Valley virus 2C and 3C inhibit type I interferon production by inducing the degradation of RIG-I. *Virology.* 2019;537:122-129.

40. Feng Q, Langereis MA, Lork M, et al. Enterovirus 2Apro targets MDA5 and MAVS in infected cells. *J Virol.* 2014;88:3369-3378.

41. Wang B, Xi X, Lei X, et al. Enterovirus 71 protease 2Apro targets MAVS to inhibit anti-viral type I interferon responses. *PLoS Pathog.* 2013;9:e1003231.

42. Zhao T, Yang L, Sun Q, et al. The NEMO adaptor bridges the nuclear factor-kappaB and interferon regulatory factor signaling pathways. *Nat Immunol.* 2007;8:592-600.

43. Wang D, Fang L, Li K, et al. Foot-and-mouth disease virus 3C protease cleaves NEMO to impair innate immune signaling. *J Virol.* 2012;86:9311-9322.

44. Wang D, Fang L, Wei D, et al. Hepatitis A virus 3C protease cleaves NEMO to impair induction of beta interferon. *J Virol.* 2014;88:10252-10258.

45. Lei X, Han N, Xiao X, Jin Q, He B, Wang J. Enterovirus 71 3C inhibits cytokine expression through cleavage of the TAK1/TAB1/TAB2/TAB3 complex. *J Virol*. 2014;88:9830-9841.

46. Dong J, Xu S, Wang J, et al. Porcine reproductive and respiratory syndrome virus 3C protease cleaves the mitochondrial antiviral signalling complex to antagonize IFN-β expression. *J Gen Virol*. 2015;96:3049-3058.

47. Lei X, Sun Z, Liu X, Jin Q, He B, Wang J. Cleavage of the adaptor protein TRIF by enterovirus 71 3C inhibits antiviral responses mediated by Toll-like receptor 3. *J Virol*. 2011;85:8811-8818.

48. Qu L, Feng Z, Yamane D, et al. Disruption of TLR3 signaling due to cleavage of TRIF by the hepatitis A virus protease-polymerase processing intermediate, 3CD. *PLoS Pathog*. 2011;7:e1002169.

49. Moustaqil M, Ollivier E, Chiu H-P, et al. SARS-CoV-2 proteases cleave IRF3 and critical modulators of inflammatory pathways (NLRP12 and TAB1): implications for disease presentation across species and the search for reservoir hosts. *BioRxiv*. 2020. https://doi.org/10.1101/2020.06.05.135699.

50. Xiang Z, Liu L, Lei X, Zhou Z, He B, Wang J. 3C protease of enterovirus D68 inhibits cellular defense mediated by interferon regulatory factor 7. *J Virol*. 2016;90:1613-1621.

51. Hung H-C, et al. Synergistic inhibition of enterovirus 71 replication by interferon and rupintrivir. *J Infect Dis*. 2011;203:1784-1790.

52. Wang H, et al. Reciprocal regulation between enterovirus 71 and the NLRP3 inflammasome. *Cell Rep*. 2015;12:42-48.

53. Wang C, et al. NLRP3 deficiency exacerbates enterovirus infection in mice. *FASEB J*. 2019;33:942-952.

54. Huang L, et al. Encephalomyocarditis virus 3C protease relieves TRAF family member-associated NF-κB activator (TANK) inhibitory effect on TRAF6-mediated NF-κB signaling through cleavage of TANK. *J Biol Chem*. 2015;290:27618-27632.

55. Lu J, et al. Enterovirus 71 disrupts interferon signaling by reducing the level of interferon receptor 1. *J Virol*. 2012;86:3767-3776.

56. Tam JCH, Bidgood SR, McEwan WA, James LC. Intracellular sensing of complement C3 activates cell autonomous immunity. *Science*. 2014;345:1256070.

57. Zhu X, Wang D, Zhou J, et al. Porcine deltacoronavirus nsp5 antagonizes type I interferon signaling by cleaving STAT2. *J Virol*. 2017;91(10):e00003–17.

58. Du Y, Bi J, Liu J, et al. 3Cpro of foot-and-mouth disease virus antagonizes the interferon signaling pathway by blocking STAT1/STAT2 nuclear translocation. *J Virol*. 2014;88:4908-4920.

59. Wang D, Dong J, Xu S, et al. Porcine epidemic diarrhea virus 3C-like protease regulates its interferon antagonism by cleaving NEMO. *J Virol*. 2016;90:2090-2101.

60. Zhu X, Wang D, Zhou J, et al. Porcine deltacoronavirus nsp5 inhibits interferon-β production through the cleavage of NEMO. *Virology*. 2017;502:33-38.

61. Huang C, Zhang Q, Guo X, et al. Porcine reproductive and respiratory syndrome virus nonstructural protein 4 antagonizes beta interferon expression by targeting the NF-κB essential modulator. *J Virol*. 2014;88:10934-10945.

62. Harris KG, Morosky SA, Drummond CG, et al. RIP3 regulates autophagy and promotes coxsackievirus B3 infection of intestinal epithelial cells. *Cell Host Microbe*. 2015;18:221-232.

63. Jagdeo JM, et al. N-terminomics TAILS identifies host cell substrates of poliovirus and coxsackievirus B3 3C proteinases that modulate virus infection. *J Virol*. 2018;92(8):e02211–17.

64. Xie L, et al. The 3C protease of enterovirus A71 counteracts the activity of host zinc-finger antiviral protein (ZAP). *J Gen Virol*. 2018;99:73-85.

65. Lei X, Zhang Z, Xiao X, et al. Enterovirus 71 inhibits pyroptosis through cleavage of gasdermin D. *J Virol*. 2017;91(18):e01069–17.

66. Mohamud Y, Qu J, Xue YC, Liu H, Deng H, Luo H. CALCOCO2/NDP52 and SQSTM1/p62 differentially regulate coxsackievirus B3 propagation. *Cell Death Differ*. 2019;26:1062-1076.

67. Shi J, Wong J, Piesik P, et al. Cleavage of sequestosome 1/p62 by an enteroviral protease results in disrupted selective autophagy and impaired NFKB signaling. *Autophagy*. 2013;9:1591-1603.

68. Corona AK, Saulsbery HM, Corona Velazquez AF, Jackson WT. Enteroviruses remodel autophagic trafficking through regulation of host SNARE proteins to promote virus replication and cell exit. *Cell Rep*. 2018;22:3304-3314.

69. Shi J, Fung G, Piesik P, Zhang J, Luo H. Dominant-negative function of the C-terminal fragments of NBR1 and SQSTM1 generated during enteroviral infection. *Cell Death Differ*. 2014;21:1432-1441.

70. Mohamud Y, Shi J, Qu J, et al. Enteroviral infection inhibits autophagic flux via disruption of the SNARE complex to enhance viral replication. *Cell Rep*. 2018;22:3292-3303.

71. Wang C, Wong J, Fung G, et al. Dysferlin deficiency confers increased susceptibility to coxsackievirus-induced cardiomyopathy. *Cell Microbiol*. 2015;17:1423-1430.

72. Badorff C, Lee GH, Lamphear BJ, et al. Enteroviral protease 2A cleaves dystrophin: evidence of cytoskeletal disruption in an acquired cardiomyopathy. *Nat Med*. 1999;5:320-326.

73. Seipelt J, Liebig HD, Sommergruber W, Gerner C, Kuechler E. 2A proteinase of human rhinovirus cleaves cytokeratin 8 in infected HeLa cells. *J Biol Chem*. 2000;275:20084-20089.

74. Joachims M, Harris KS, Etchison D. Poliovirus protease 3C mediates cleavage of microtubule-associated protein 4. *Virology*. 1995;211:451-461.

75. Yalamanchili P, Weidman K, Dasgupta A. Cleavage of transcriptional activator Oct-1 by poliovirus encoded protease 3Cpro. *Virology*. 1997;239:176-185.

76. Shiroki K, Isoyama T, Kuge S, et al. Intracellular redistribution of truncated La protein produced by poliovirus 3Cpro-mediated cleavage. *J Virol*. 1999;73:2193-2200.

77. Clark ME, Lieberman PM, Berk AJ, Dasgupta A. Direct cleavage of human TATA-binding protein by poliovirus protease 3C in vivo and in vitro. *Mol Cell Biol*. 1993;13:1232-1237.

78. Kundu P, Raychaudhuri S, Tsai W, Dasgupta A. Shutoff of RNA polymerase II transcription by poliovirus involves 3C protease-mediated cleavage of the TATA-binding protein at an alternative site: incomplete shutoff of transcription interferes with efficient viral replication. *J Virol*. 2005;79:9702-9713.

79. Das S, Dasgupta A. Identification of the cleavage site and determinants required for poliovirus 3CPro-catalyzed cleavage of human TATA-binding transcription factor TBP. *J Virol*. 1993;67:3326-3331.

80. Clark ME, Hämmerle T, Wimmer E, Dasgupta A. Poliovirus proteinase 3C converts an active form of transcription factor IIIC to an inactive form: a mechanism for inhibition of host cell polymerase III transcription by poliovirus. *EMBO J*. 1991;10:2941-2947.

81. Yalamanchili P, Datta U, Dasgupta A. Inhibition of host cell transcription by poliovirus: cleavage of transcription factor CREB by poliovirus-encoded protease 3Cpro. *J Virol*. 1997;71:1220-1226.

82. Yalamanchili P, Harris K, Wimmer E, Dasgupta A. Inhibition of basal transcription by poliovirus: a virus- encoded protease (3Cpro) inhibits formation of TBP-TATA box complex in vitro. *J Virol*. 1996;70:2922-2929.

83. Wong J, Zhang J, Yanagawa B, et al. Cleavage of serum response factor mediated by enteroviral protease 2A contributes to impaired cardiac function. *Cell Res*. 2012;22:360-371.

84. Back SH, Kim YK, Kim WJ, et al. Translation of polioviral mRNA is inhibited by cleavage of polypyrimidine tract-binding proteins executed by polioviral 3C(pro). *J Virol*. 2002;76:2529-2542.

85. Jagdeo JM, Dufour A, Fung G, et al. Heterogeneous nuclear ribonucleoprotein M facilitates enterovirus infection. *J Virol.* 2015;89:7064-7078.

86. Almstead LL, Sarnow P. Inhibition of U snRNP assembly by a virus-encoded proteinase. *Genes Dev.* 2007;21:1086-1097.

87. Fung G, Shi J, Deng H, et al. Cytoplasmic translocation, aggregation, and cleavage of TDP-43 by enteroviral proteases modulate viral pathogenesis. *Cell Death Differ.* 2015;22:2087-2097.

88. Neznanov N, Chumakov KM, Neznanova L, Almasan A, Banerjee AK, Gudkov AV. Proteolytic cleavage of the p65-RelA subunit of NF-kappaB during poliovirus infection. *J Biol Chem.* 2005;280:24153-24158.

89. Wong J, Si X, Angeles A, et al. Cytoplasmic redistribution and cleavage of AUF1 during coxsackievirus infection enhance the stability of its viral genome. *FASEB J.* 2013;27:2777-2787.

90. Joachims M, Van Breugel PC, Lloyd RE. Cleavage of poly(A)-binding protein by enterovirus proteases concurrent with inhibition of translation in vitro. *J Virol.* 1999;73:718-727.

91. Sun D, Wang M, Wen X, et al. Cleavage of poly(A)-binding protein by duck hepatitis A virus 3C protease. *Sci Rep.* 2017;7:16261.

92. Zhang B, Morace G, Gauss-Müller V, Kusov Y. Poly(A) binding protein, C-terminally truncated by the hepatitis A virus proteinase 3C, inhibits viral translation. *Nucleic Acids Res.* 2007;35:5975-5984.

93. Kobayashi M, Arias C, Garabedian A, Palmenberg AC, Mohr I. Site-specific cleavage of the host poly(A) binding protein by the encephalomyocarditis virus 3C proteinase stimulates viral replication. *J Virol.* 2012;86:10686-10694.

94. Belsham GJ, McInerney GM, Ross-Smith N. Foot-and-mouth disease virus 3C protease induces cleavage of translation initiation factors eIF4A and eIF4G within infected cells. *J Virol.* 2000;74:272-280.

95. Devaney MA, Vakharia VN, Lloyd RE, Ehrenfeld E, Grubman MJ. Leader protein of foot-and-mouth disease virus is required for cleavage of the p220 component of the cap-binding protein complex. *J Virol.* 1988;62:4407-4409.

96. Medina M, Domingo E, Brangwyn JK, Belsham GJ. The two species of the foot-and-mouth disease virus leader protein, expressed individually, exhibit the same activities. *Virology.* 1993;194:355-359.

97. Chau DHW, Zhang H, Yuan J, et al. Coxsackievirus B3 proteases 2A and 3C induce apoptotic cell death through mitochondrial injury and cleavage of eIF4GI but not DAP5/p97/NAT1. *Apoptosis.* 2007;12:513-524.

98. Lamphear BJ, Rhoads RE. A single amino acid change in protein synthesis initiation factor 4G renders cap-dependent translation resistant to picornaviral 2A proteases. *Biochemistry.* 1996;35:15726-15733.

99. Lamphear BJ, Kirchweger R, Skern T, Rhoads RE. Mapping of functional domains in eukaryotic protein synthesis initiation factor 4G (eIF4G) with picornaviral proteases. Implications for cap-dependent and cap-independent translational initiation. *J Biol Chem.* 1995;270:21975-21983.

100. de Breyne S, Bonderoff JM, Chumakov KM, Lloyd RE, Hellen CUT. Cleavage of eukaryotic initiation factor eIF5B by enterovirus 3C proteases. *Virology.* 2008;378:118-122.

101. Hanson PJ, Ye X, Qiu Y, et al. Cleavage of DAP5 by coxsackievirus B3 2A protease facilitates viral replication and enhances apoptosis by altering translation of IRES-containing genes. *Cell Death Differ.* 2016;23:828-840.

102. Perera R, Daijogo S, Walter BL, Nguyen JHC, Semler BL. Cellular protein modification by poliovirus: the two faces of poly(rC)-binding protein. *J Virol.* 2007;81:8919-8932.

103. Dougherty JD, White JP, Lloyd RE. Poliovirus-mediated disruption of cytoplasmic processing bodies. *J Virol.* 2011;85:64-75.

104. Zaragoza C, Saura M, Padalko EY, et al. Viral protease cleavage of inhibitor of kappaBalpha triggers host cell apoptosis. *Proc Natl Acad Sci USA.* 2006;103:19051-19056.

105. Deng H, Fung G, Shi J, et al. Enhanced enteroviral infectivity via viral protease-mediated cleavage of Grb2-associated binder 1. *FASEB J.* 2015;29:4523-4531.

106. Park N, Skern T, Gustin KE. Specific cleavage of the nuclear pore complex protein Nup62 by a viral protease. *J Biol Chem.* 2010;285:28796-28805.

107. Watters K, Palmenberg AC. Differential processing of nuclear pore complex proteins by rhinovirus 2A proteases from different species and serotypes. *J Virol.* 2011;85:10874-10883.

108. Fung G, Ng CS, Zhang J, et al. Production of a dominant-negative fragment due to G3BP1 cleavage contributes to the disruption of mitochondria-associated protective stress granules during CVB3 infection. *PLoS One.* 2013;8:e79546.

109. Ng CS, Jogi M, Yoo J-S, et al. Encephalomyocarditis virus disrupts stress granules, the critical platform for triggering antiviral innate immune responses. *J Virol.* 2013;87:9511-9522.

110. White JP, Cardenas AM, Marissen WE, Lloyd RE. Inhibition of cytoplasmic mRNA stress granule formation by a viral proteinase. *Cell Host Microbe.* 2007;2:295-305.

111. Ye X, Pan T, Wang D, et al. Foot-and-Mouth disease virus counteracts on internal ribosome entry site suppression by G3BP1 and inhibits G3BP1-mediated stress granule assembly via post-translational mechanisms. *Front Immunol.* 2018;9:1142.

112. Visser LJ, Langereis MA, Rabouw HH, et al. Essential role of enterovirus 2A protease in counteracting stress granule formation and the induction of type I interferon. *J Virol.* 2019;93.

113. Visser LJ, Medina GN, Rabouw HH, et al. Foot-and-Mouth disease virus leader protease cleaves G3BP1 and G3BP2 and inhibits stress granule formation. *J Virol.* 2019;93.

114. Ullah MO, Sweet MJ, Mansell A, Kellie S, Kobe B. TRIF-dependent TLR signaling, its functions in host defense and inflammation, and its potential as a therapeutic target. *J Leukoc Biol.* 2016;100:27-45.

115. Xu C, He X, Zheng Z, et al. Downregulation of microRNA miR-526a by enterovirus inhibits RIG-I-dependent innate immune response. *J Virol.* 2014;88:11356-11368.

116. Zhang M, et al. Regulation of IkappaB kinase-related kinases and antiviral responses by tumor suppressor CYLD. *J Biol Chem.* 2008;283:18621-18626.

117. Zeng, W et al. Reconstitution of the RIG-I pathway reveals a signaling role of unanchored polyubiquitin chains in innate immunity. *Cell.* 2010;141:315–330.

118. Chan RWY, et al. Tropism of and innate immune responses to the novel human betacoronavirus lineage C virus in human ex vivo respiratory organ cultures. *J Virol.* 2013;87:6604-6614.

119. Menachery VD, et al. Pathogenic influenza viruses and coronaviruses utilize similar and contrasting approaches to control interferon-stimulated gene responses. *MBio.* 2014;5:e01174-e011714.

120. Zhou J, et al. Active replication of Middle East respiratory syndrome coronavirus and aberrant induction of inflammatory cytokines and chemokines in human macrophages: implications for pathogenesis. *J Infect Dis.* 2014;209:1331-1342.

121. Channappanavar R, et al. Dysregulated type I interferon and inflammatory monocyte-macrophage responses cause lethal pneumonia in SARS-CoV-infected mice. *Cell Host Microbe.* 2016;19:181-193.

122. Blanco-Melo D, et al. Imbalanced Host Response to SARS-CoV-2 Drives Development of COVID-19. *Cell.* 2020;181:1036-1045 e9.

123. Lokugamage KG, Hage A, Vries MD, et al. Type I interferon susceptibility distinguishes SARS-CoV-2 from SARS-CoV. *J Virol.* 2020;94(23):e01410–e01420. https://doi.org/10.1128/JVI.01410-20.

124. Clementz MA, et al. Deubiquitinating and interferon antagonism activities of coronavirus papain-like proteases. *J Virol.* 2010; 84:4619-4629.

125. Matthews K, Schäfer A, Pham A, Frieman M. The SARS coronavirus papain like protease can inhibit IRF3 at a post activation step that requires deubiquitination activity. *Virol J.* 2014;11:209.

126. Kopecky-Bromberg SA, Martínez-Sobrido L, Frieman M, Baric RA, Palese P. Severe acute respiratory syndrome coronavirus open reading frame (ORF) 3b, ORF 6, and nucleocapsid proteins function as interferon antagonists. *J Virol.* 2007;81:548-557.

127. Siu K-L, et al. Severe acute respiratory syndrome coronavirus M protein inhibits type I interferon production by impeding the formation of TRAF3.TANK.TBK1/IKKepsilon complex. *J Biol Chem.* 2009;284:16202-16209.

128. Onomoto K, et al. Critical role of an antiviral stress granule containing RIG-I and PKR in viral detection and innate immunity. *PLoS One.* 2012;7:e43031.

129. Kim SS-Y, Sze L, Liu C, Lam K-P. The stress granule protein G3BP1 binds viral dsRNA and RIG-I to enhance interferon-β response. *J Biol Chem.* 2019;294:6430-6438.

130. Kuniyoshi K, et al. Pivotal role of RNA-binding E3 ubiquitin ligase MEX3C in RIG-I-mediated antiviral innate immunity. *Proc Natl Acad Sci USA.* 2014;111:5646-5651.

131. Narita R, et al. A novel function of human Pumilio proteins in cytoplasmic sensing of viral infection. *PLoS Pathog.* 2014;10: e1004417.

132. Yoo J-S, et al. DHX36 enhances RIG-I signaling by facilitating PKR-mediated antiviral stress granule formation. *PLoS Pathog.* 2014;10: e1004012.

133. Cheng J, Gao S, Zhu C, et al. Typical stress granule proteins interact with the 3' untranslated region of enterovirus D68 to inhibit viral replication. *J Virol.* 2020;94(7):e02041–17.

134. Rabouw HH, et al. Middle East respiratory coronavirus accessory protein 4a inhibits PKR-mediated antiviral stress responses. *PLoS Pathog.* 2016;12:e1005982.

135. Nakagawa K, Narayanan K, Wada M, Makino S. Inhibition of stress granule formation by middle east respiratory syndrome coronavirus 4a accessory protein facilitates viral translation, leading to efficient virus replication. *J Virol.* 2018;92(20):e00902–18.

136. Icardi L, et al. Opposed regulation of type I IFN-induced STAT3 and ISGF3 transcriptional activities by histone deacetylases (HDACS) 1 and 2. *FASEB J.* 2012;26:240-249.

137. Klampfer L, Huang J, Swaby L-A, Augenlicht L. Requirement of histone deacetylase activity for signaling by STAT1. *J Biol Chem.* 2004;279:30358-30368.

138. Reineke LC, Lloyd RE. The stress granule protein G3BP1 recruits protein kinase R to promote multiple innate immune antiviral responses. *J Virol.* 2015;89:2575-2589.

139. Chen N, et al. Epidemiological and clinical characteristics of 99 cases of 2019 novel coronavirus pneumonia in Wuhan, China: a descriptive study. *Lancet.* 2020;395:507-513.

140. Zhou F, et al. Clinical course and risk factors for mortality of adult inpatients with COVID-19 in Wuhan, China: a retrospective cohort study. *Lancet.* 2020;395:1054-1062.

141. Hyun J, Kanagavelu S, Fukata M. A unique host defense pathway: TRIF mediates both antiviral and antibacterial immune responses. *Microbes Infect.* 2013;15:1-10.

142. Hu S, et al. PKR-dependent cytosolic cGAS foci are necessary for intracellular DNA sensing. *Sci Signal.* 2019;12.

143. Liu Z-S, et al. G3BP1 promotes DNA binding and activation of cGAS. *Nat Immunol.* 2019;20:18-28.

144. Li X-D, et al. Pivotal roles of cGAS-cGAMP signaling in antiviral defense and immune adjuvant effects. *Science.* 2013;341:1390-1394.

145. Zhao C, Zhao W. NLRP3 inflammasome-A key player in antiviral responses. *Front Immunol.* 2020;11:211.

146. Shi J, et al. Cleavage of GSDMD by inflammatory caspases determines pyroptotic cell death. *Nature.* 2015;526:660-665.

147. Liu X, et al. Inflammasome-activated gasdermin D causes pyroptosis by forming membrane pores. *Nature.* 2016;535:153-158.

148. Wang X, et al. RNA viruses promote activation of the NLRP3 inflammasome through a RIP1-RIP3-DRP1 signaling pathway. *Nat Immunol.* 2014;15:1126-1133.

149. Negash AA, et al. IL-1β production through the NLRP3 inflammasome by hepatic macrophages links hepatitis C virus infection with liver inflammation and disease. *PLoS Pathog.* 2013;9:e1003330.

150. Tschöpe C, Muller I, Xia Y, et al. NOD2 (nucleotide-binding oligomerization domain 2) is a major pathogenic mediator of coxsackievirus B3-induced myocarditis. *Circ Heart Fail*; 2017;10(9): e003870.

151. Wang Y, Gao B, Xiong S. Involvement of NLRP3 inflammasome in CVB3-induced viral myocarditis. *Am J Physiol Heart Circ Physiol.* 2014;307:H1438-H1447.

152. Chen G, Wu D, Guo W, et al. Clinical and immunological features of severe and moderate coronavirus disease 2019. *J Clin Invest.* 2020;130:2620-2629.

153. Siu K-L, Yuen K-S, Castaño-Rodriguez C, et al. Severe acute respiratory syndrome coronavirus ORF3a protein activates the NLRP3 inflammasome by promoting TRAF3-dependent ubiquitination of ASC. *FASEB J.* 2019;33:8865-8877.

154. Shi C-S, Nabar NR, Huang N-N, Kehrl JH. SARS-Coronavirus Open Reading Frame-8b triggers intracellular stress pathways and activates NLRP3 inflammasomes. *Cell Death Discov.* 2019;5:101.

155. Nieto-Torres JL, Verdiá-Báguena C, Jimenez-Guardeño JM, et al. Severe acute respiratory syndrome coronavirus E protein transports calcium ions and activates the NLRP3 inflammasome. *Virology.* 2015;485;330–339.

156. Rodrigues TS, Sa KS, Ishimoto AY, et al. Inflammasome activation in COVID-19 patients. *medRxiv.* 2020. https://doi.org/10.1101/2020. 08.05.20168872.

157. Tsai W-C, Lloyd RE. Cytoplasmic RNA granules and viral infection. *Annu Rev Virol.* 2014;1:147-170.

158. Abernathy E, Glaunsinger B. Emerging roles for RNA degradation in viral replication and antiviral defense. *Virology.* 2015:479-480;600-608.

159. Ng CS, Kasumba DM, Fujita T, Luo H. Spatio-temporal characterization of the antiviral activity of the XRN1-DCP1/2 aggregation against cytoplasmic RNA viruses to prevent cell death. *Cell Death Differ.* 2020;27:2363-2382.

160. Cencic R, Desforges M, Hall DR, et al. Blocking eIF4E-eIF4G interaction as a strategy to impair coronavirus replication. *J Virol.* 2011;85:6381-6389.

161. Cencic R, Hall DR, Robert F, et al. Reversing chemoresistance by small molecule inhibition of the translation initiation complex eIF4F. *Proc Natl Acad Sci USA.* 2011;108:1046-1051.

162. Galluzzi L, Baehrecke EH, Ballabio A, et al. Molecular definitions of autophagy and related processes. *Embo J.* 2017;36:1811-1836.

163. Deretic V, Saitoh T, Akira S. Autophagy in infection, inflammation and immunity. *Nat Rev Immunol.* 2013;13:722-737.

164. Deretic V, Levine B. Autophagy balances inflammation in innate immunity. *Autophagy.* 2018;14:243-251.

165. Kim B-W, Kwon DH, Song HK. Structure biology of selective autophagy receptors. *BMB Rep.* 2016;49:73-80.

166. Mohamud Y, Luo H. The intertwined life cycles of enterovirus and autophagy. *Virulence.* 2019;10:470-480.

167. Kubli DA, Gustafsson ÅB. Mitochondria and mitophagy: the yin and yang of cell death control. *Circ Res.* 2012;111:1208-1221.

168. Nakamura S, Yoshimori T. New insights into autophagosome-lysosome fusion. *J Cell Sci*. 2017;130:1209-1216.

169. Gassen NC, Papies J, Bajaj T, et al. Analysis of SARS-CoV-2-controlled autophagy reveals spermidine, MK-2206, and niclosamide as putative antiviral therapeutics. *BioRxiv*. 2020. https://doi.org/10.1101/2020.04.15.997254.

170. Gassen NC, Niemeyer D, Muth D, et al. SKP2 attenuates autophagy through Beclin1-ubiquitination and its inhibition reduces MERS-Coronavirus infection. *Nat Commun*. 2019;10:5770.

171. Chen X, Wang K, Xing Y, et al. Coronavirus membrane-associated papain-like proteases induce autophagy through interacting with Beclin1 to negatively regulate antiviral innate immunity. *Protein Cell*. 2014;5:912-927.

172. Kleifeld O, Doucet A, Prudova A, et al. Identifying and quantifying proteolytic events and the natural N terminome by terminal amine isotopic labeling of substrates. *Nat Protoc*. 2011;6:1578-1611.

173. Schilling O, Overall CM. Proteome-derived, database-searchable peptide libraries for identifying protease cleavage sites. *Nat Biotechnol*. 2008;26:685-694.

174. Schilling O, Huesgen PF, Barré O. Auf dem Keller U, Overall C M. Characterization of the prime and non-prime active site specificities of proteases by proteome-derived peptide libraries and tandem mass spectrometry. *Nat Protoc*. 2011;6:111-120.

175. Kleifeld O, Doucet A, auf dem Keller U, et al. Isotopic labeling of terminal amines in complex samples identifies protein N-termini and protease cleavage products. *Nat Biotechnol*. 2010;28:281-288.

176. Huesgen PF, Overall CM. N- and C-terminal degradomics: new approaches to reveal biological roles for plant proteases from substrate identification. *Physiol Plant*. 2012;145:5-17.

177. Klein T, Fung S-Y, Renner F, et al. The paracaspase MALT1 cleaves HOIL1 reducing linear ubiquitination by LUBAC to dampen lymphocyte NF-κB signalling. *Nat Commun*. 2015;6:8777.

178. Eckhard U, Bandukwala H, Mansfield MJ, et al. Discovery of a proteolytic flagellin family in diverse bacterial phyla that assembles enzymatically active flagella. *Nat Commun*. 2017;8:521.

179. Pillaiyar T, Manickam M, Namasivayam V, Hayashi Y, Jung S-H. An overview of severe acute respiratory syndrome-coronavirus (SARS-CoV) 3CL protease inhibitors: peptidomimetics and small molecule chemotherapy. *J Med Chem*. 2016;59:6595-6628.

180. Lu G, Qi J, Chen Z, et al. Enterovirus 71 and coxsackievirus A16 3C proteases: binding to rupintrivir and their substrates and anti-hand, foot, and mouth disease virus drug design. *J Virol*. 2011;85:10319-10331.

181. Binford SL, Maldonado F, Brothers MA, et al. Conservation of amino acids in human rhinovirus 3C protease correlates with broad-spectrum antiviral activity of rupintrivir, a novel human rhinovirus 3C protease inhibitor. *Antimicrob Agents Chemother*. 2005;49:619-626.

182. Tan J, George S, Kusov Y, et al. 3C protease of enterovirus 68: structure-based design of Michael acceptor inhibitors and their broad-spectrum antiviral effects against picornaviruses. *J Virol*. 2013;87:4339-4351.

183. van der Linden L, Ulferts R, Nabuurs SB, et al. Application of a cell-based protease assay for testing inhibitors of picornavirus 3C proteases. *Antiviral Res*. 2014;103:17-24.

184. Yang H, Xie W, Xue X, et al. Design of wide-spectrum inhibitors targeting coronavirus main proteases. *PLoS Biol*. 2005;3:e324.

185. Hayden FG, Turner RB, Gwaltney JM, et al. Phase II, randomized, double-blind, placebo-controlled studies of ruprintrivir nasal spray 2-percent suspension for prevention and treatment of experimentally induced rhinovirus colds in healthy volunteers. *Antimicrob Agents Chemother*. 2003;47:3907-3916.

186. Grein J, Ohmagari N, Shin D, et al. Compassionate Use of Remdesivir for Patients with Severe Covid-19. *N Engl J Med*. 2020;382(24):2327–2336. https://doi.org/10.1056/nejmoa2007016.

187. Touret F, de Lamballerie X. Of chloroquine and COVID-19. *Antiviral Res*. 2020;177:104762.

188. Wang M, Cao R, Zhang L, et al. Remdesivir and chloroquine effectively inhibit the recently emerged novel coronavirus (2019-nCoV) in vitro. *Cell Research*. 2020;30(3):269–271. https://doi.org/10.1038/s41422-020-0282-0.

189. Hoffmann M, Mösbauer K, Hofmann-Winkler H, et al. Chloroquine does not inhibit infection of human lung cells with SARS-CoV-2. *Nature*. 2020;585(7826):588–590. https://doi.org/10.1038/s41586-020-2575-3.

190. Chorin E, Rozenbaum Z, Topilsky Y, et al. Tricuspid regurgitation and long-term clinical outcomes. *European Heart Journal - Cardiovascular Imaging*. 2019;21:157–165. https://doi.org/10.1093/ehjci/jez216.

191. Yang S, Chen S-J, Hsu M-F, et al. Synthesis, crystal structure, structure-activity relationships, and antiviral activity of a potent SARS coronavirus 3CL protease inhibitor. *J Med Chem*. 2006;49:4971-4980.

192. Jo S, Kim S, Shin DH, Kim M-S. Inhibition of SARS-CoV 3CL protease by flavonoids. *J Enzyme Inhib Med Chem*. 2020;35:145-151.

193. Ramajayam R, Tan K-P, Liu H-G, Liang P-H. Synthesis and evaluation of pyrazolone compounds as SARS-coronavirus 3C-like protease inhibitors. *Bioorg Med Chem*. 2010;18:7849-7854.

194. Zhang J, Huitema C, Niu C, et al. Aryl methylene ketones and fluorinated methylene ketones as reversible inhibitors for severe acute respiratory syndrome (SARS) 3C-like proteinase. *Bioorg Chem*. 2008;36:229-240.

195. Blanchard JE, Elowe NH, Huitema C, et al. High-throughput screening identifies inhibitors of the SARS coronavirus main proteinase. *Chem. Biol*. 2004;11:1445-1453.

196. Wu C-Y, King K-Y, Kuo C-J, et al. Stable benzotriazole esters as mechanism-based inactivators of the severe acute respiratory syndrome 3CL protease. *Chem. Biol*. 2006;13:261-268.

197. Verschueren KHG, Pumpor K, Anemüller S, Chen S, Mesters JR, Hilgenfeld R. A structural view of the inactivation of the SARS coronavirus main proteinase by benzotriazole esters. *Chem. Biol*. 2008;15:597-606.

198. Bacha U, Barrila J, Velazquez-Campoy A, Leavitt SA, Freire E. Identification of novel inhibitors of the SARS coronavirus main protease 3CLpro. *Biochemistry*. 2004;43:4906-4912.

199. Lee T-W, Cherney MM, Liu J, et al. Crystal structures reveal an induced-fit binding of a substrate-like Aza-peptide epoxide to SARS coronavirus main peptidase. *J Mol Biol*. 2007;366:916-932.

200. Lee T-W, Cherney MM, Huitema C, et al. Crystal structures of the main peptidase from the SARS coronavirus inhibited by a substrate-like aza-peptide epoxide. *J Mol Biol*. 2005;353:1137-1151.

201. Asgian JL, James KE, Li ZZ, et al. Aza-peptide epoxides: a new class of inhibitors selective for clan CD cysteine proteases. *J Med Chem*. 2002;45:4958-4960.

202. Kaeppler U, Stiefl N, Schiller M, et al. A new lead for nonpeptidic active-site-directed inhibitors of the severe acute respiratory syndrome coronavirus main protease discovered by a combination of screening and docking methods. *J Med Chem*. 2005;48:6832-6842.

203. Kaeppler U, Schirmeister T. New non-peptidic inhibitors of papain derived from etacrynic acid. *Med Chem*. 2005;1:361-370.

204. Shao Y-M, Yang W-B, Peng H-P, et al. Structure-based design and synthesis of highly potent SARS-CoV 3CL protease inhibitors. *Chembiochem*. 2007;8:1654-1657.

205. Tsai K-C, Chen S-Y, Liang P-H, et al. Discovery of a novel family of SARS-CoV protease inhibitors by virtual screening and 3D-QSAR studies. *J Med Chem*. 2006;49:3485-3495.

206. Lu I-L, Mahindroo N, Liang P-H, et al. Structure-based drug design and structural biology study of novel nonpeptide inhibitors of severe acute respiratory syndrome coronavirus main protease. *J Med Chem.* 2006;49:5154-5161.

207. Ghosh AK, Xi K, Ratia K, et al. Design and synthesis of peptidomimetic severe acute respiratory syndrome chymotrypsin-like protease inhibitors. *J Med Chem.* 2005;48:6767-6771.

208. Shie J-J, Fang J-M, Kuo T-H, et al. Inhibition of the severe acute respiratory syndrome 3CL protease by peptidomimetic alpha,beta-unsaturated esters. *Bioorg Med Chem.* 2005;13:5240-5252.

209. Ryu YB, Jeong HJ, Kim JH, et al. Biflavonoids from Torreya nucifera displaying SARS-CoV 3CL(pro) inhibition. *Bioorg Med Chem.* 2010;18:7940-7947.

210. Wen C-C, Kuo Y-H, Jan J-T, et al. Specific plant terpenoids and lignoids possess potent antiviral activities against severe acute respiratory syndrome coronavirus. *J Med Chem.* 2007;50:4087-4095.

211. Ryu YB, Park S-J, Kim YM, et al. SARS-CoV 3CLpro inhibitory effects of quinone-methide triterpenes from Tripterygium regelii. *Bioorg Med Chem Lett.* 2010;20:1873-1876.

212. Lee C-C, Kuo C-J, Hsu M-F, et al. Structural basis of mercury- and zinc-conjugated complexes as SARS-CoV 3C-like protease inhibitors. *FEBS Lett.* 2007;581:5454-5458.

213. Hsu JT-A, Kuo C-J, Hsieh H-P, et al. Evaluation of metal-conjugated compounds as inhibitors of 3CL protease of SARS-CoV. *FEBS Lett.* 2004;574:116-120.

214. Zhang L, Lin D, Kusov Y, et al. α-Ketoamides as broad-spectrum inhibitors of coronavirus and enterovirus replication: structure-based design, synthesis, and activity assessment. *J Med Chem.* 2020;63:4562-4578.

215. Jacobs J, Grum-Tokars V, Zhou Y, et al. Discovery, synthesis, and structure-based optimization of a series of N-(tert-butyl)-2-(N-arylamido)-2-(pyridin-3-yl) acetamides (ML188) as potent noncovalent small molecule inhibitors of the severe acute respiratory syndrome coronavirus (SARS-CoV) 3CL protease. *J Med Chem.* 2013;56:534-546.

216. Turlington M, et al. Discovery of N-(benzo[1,2,3]triazol-1-yl)-N-(benzyl)acetamido)phenyl carboxamides as severe acute respiratory syndrome coronavirus (SARS-CoV) 3CLpro inhibitors: identification of ML300 and noncovalent nanomolar inhibitors with an induced-fit binding. *Bioorg Med Chem Lett.* 2013;23:6172-6177.

217. Barretto N, et al. The papain-like protease of severe acute respiratory syndrome coronavirus has deubiquitinating activity. *J Virol.* 2005;79:15189-15198.

218. Dragovich PS, et al. Structure-based design, synthesis, and biological evaluation of irreversible human rhinovirus 3C protease inhibitors. 4. Incorporation of P1 lactam moieties as L-glutamine replacements. *J Med Chem.* 1999;42:1213-1224.

219. Yuan S, et al. Structure of the HRV-C 3C-rupintrivir complex provides new insights for inhibitor design. *Virol Sin.* 2020;35:445–454. https://doi.org/10.1007/s12250-020-00196-4.

220. Ma C, et al. Boceprevir, GC-376, and calpain inhibitors II, XII inhibit SARS-CoV-2 viral replication by targeting the viral main protease. *Cell Res.* 2020;30:678–692. https://doi.org/10.1038/s41422-020-0356-z.

221. Kuo C-J, Shie J-J, Fang J-J, et al. Design, synthesis, and evaluation of 3C protease inhibitors as anti-enterovirus 71 agents. *Bioorg Med Chem.* 2008;16:7388-7398.

222. Morse JS, Lalonde T, Xu S, Liu WR. Learning from the past: possible urgent prevention and treatment options for severe acute respiratory infections caused by 2019-nCoV. *Chembiochem.* 2020;21:730-738.

223. Liu W, Zhu H-M, Niu G-J, et al. Synthesis, modification and docking studies of 5-sulfonyl isatin derivatives as SARS-CoV 3C-like protease inhibitors. *Bioorg Med Chem.* 2014;22:292-302.

224. Chen L-R, Wang Y-C, Lin YW, et al. Synthesis and evaluation of isatin derivatives as effective SARS coronavirus 3CL protease inhibitors. *Bioorg Med Chem Lett.* 2005;15:3058-3062.

225. Shie J-J, Fang J-M, Kuo C-J, et al. Discovery of potent anilide inhibitors against the severe acute respiratory syndrome 3CL protease. *J Med Chem.* 2005;48:4469-4473.

226. Sang P, Tian S, Meng Z, Yang L. Insight derived from molecular docking and molecular dynamics simulations into the binding interactions between HIV-1 protease inhibitors and SARS-CoV-2 3CLpro. 2020. https://doi.org/10.26434/chemrxiv.11932995.v1.

227. Shimamoto Y, Hattori Y, Kobayashi K, et al. Fused-ring structure of decahydroisoquinolin as a novel scaffold for SARS 3CL protease inhibitors. *Bioorg Med Chem.* 2015;23:876-890.

228. Zhang H-Z, Zhang H, Kemnitzer W, et al. Design and synthesis of dipeptidyl glutaminyl fluoromethyl ketones as potent severe acute respiratory syndrome coronovirus (SARS-CoV) inhibitors. *J Med Chem.* 2006;49:1198-1201.